Approximating Complex Pareto Fronts with Pre-defined Normal-Boundary Intersection Directions

Maha Elarbi, Slim Bechikh, Carlos A. Coello Coello, *Fellow, IEEE*, and Lamjed Ben Said

***Abstract*—Decomposition-based evolutionary algorithms using pre-defined reference points have shown good performance in many-objective optimization. Unfortunately, almost all experimental studies have focused on problems having regular PFs (Pareto Fronts). Recently, it has been shown that the performance of such algorithms is deteriorated when facing irregular PFs such as degenerate, discontinuous, inverted, strongly convex, and/or strongly concave fronts. The main issue is that the pre-defined reference points may not all intersect with the PF. Therefore, many researchers proposed to update the reference points with the aim of adapting them to the discovered Pareto shape. Unfortunately, the adaptive update does not really solve the issue for two main reasons. On the one hand, there is a considerable difficulty to set the time and the frequency of updates. On the other hand, it is not easy to define how to update the search directions for an unknown PF shape. This paper proposes to approximate irregular PFs using a set of pre-defined NBI (Normal-Boundary Intersection) directions. The main motivation behind our work is that when using a set of well-distributed NBI directions, all these directions intersect with the PF regardless of its shape, except for the case of discontinuous and/or degenerate fronts. To handle the latter cases, a simple interaction mechanism between the Decision Maker (DM) and the algorithm is used. In fact, the DM is asked if the number of NBI directions needs to be increased in some stages of the evolutionary process. If so, the resolution of the NBI directions that intersect the PF is increased to properly cover discontinuous and/or degenerate PFs. Our experimental results on benchmark problems with regular and irregular PFs, having up to fifteen objectives, show the merits of our algorithm when compared to five of the most representative state-of-the-art algorithms including two adaptive approaches.**

***Index Terms*—Irregular Pareto fronts, decomposition, normal-boundary intersection directions, evolutionary many-objective optimization**

I. Introduction

RECENTLY, Multi-objective Optimization Problems (MOPs) characterized with more than three conflicting objectives known as Many-objective Optimization Problems (MaOPs) have gained a wide interest [1], [2], [3]. A variety of real-world applications involving a high number of objectives are also available, e.g., in airfoil design [4], water distribution system design [5], and engineering design [6]. Hence, much effort needs to be devoted in order to design effective optimizers to solve MaOPs. Moreover, the classical existing Pareto-dominance based Multi-Objective Evolutionary Algorithms (MOEAs)[7], [8] have encountered many difficulties in solving MaOPs. In spite of their popularity, Pareto-based MOEAs are known to suffer from some drawbacks when dealing with MaOPs [9], [10]. Thus, commendable efforts have been made by the Evolutionary Multi-objective Optimization (EMO) community to design new Many-Objective Evolutionary Algorithms (MaOEAs) for solving problems having more than three objectives [11], [12], [13], [14], [15], [16], [17].

Recently, a number of MaOEAs have shown good performance on benchmark problems with regular Pareto Fronts (PFs). Note that evolutionary many-objective optimization is a new avenue of research. Hence, great improvements in dealing with irregular PFs are still needed to design effective MaOEAs. Besides, problems characterized with irregular PFs pose an additional challenges for decomposition-based MaOEAs that employ a pre-defined set of reference points since their performance strongly depend on the shape of the PF [18]. In fact, when facing a problem with highly irregular PF, the pre-defined reference points may not all intersect the PF. Hence, we cannot guarantee that the reference points uniformly intersect the PF. In addition, although various decomposition-based MaOEAs have been proposed, most of them employ the Penalty-based Boundary Intersection (PBI) scalarizing function [12] with a penalty parameter $\theta = 5.0$. Ishibuchi et al. [19] have shown that using PBI with $\theta = 0.1$ outperforms the results obtained with $\theta = 5.0$ when solving multi-objective knapsack problems. Hence, the value of the θ parameter is problem dependent [20], [21].

Those observations greatly motivated us to introduce a Mirror Point-based Relation (MPR). In MPR, two sets of directions are employed. The PBI directions are used to ensure the diversity of the population, while the NBI directions guarantee the uniformity since they intersect the PF regardless of its shape [22]. An environmental selection strategy based on the MPR is conducted to select the solutions, referred to as MPR-based Selection Strategy (MPRSS). The MPRSS is incorporated into the framework of θ-DEA to give rise to MP-DEA (Mirror Point Decomposition-based Evolutionary Algorithm). The final contribution of this paper is that we conduct extensive comparative experiments against five recently proposed decomposition-based MaOEAs on the DTLZ1-4

Maha Elarbi, Slim Bechikh, and Lamjed Ben Said are with the Strategies for Modelling and ARtificial inTelligence (SMART) Laboratory, ISG-Tunis, University of Tunis (Université de Tunis), Tunis 2000, Tunisia (e-mail: arbi.maha@yahoo.com, slim.bechikh@fsegn.rnu.tn, lamjed.bensaid@isg.rnu.tn).

C.A. Coello Coello is with UAM-Azcapotzalco, Departamento de Sistemas, Mexico City, MEXICO. He is on sabbatical leave from CINVESTAV-IPN, Department of Computer Science (Evolutionary Computation Group), Mexico City 07300, MEXICO. E-mail: ccoello@cs.cinvestav.mx. He gratefully acknowledges support from CONACyT grant no. 2016-01-1920 (Fronteras de la Ciencia).

[23], inverted DTLZ1-4 [9], WFG1-9 [24], and six MaF [25] benchmark suites with up to fifteen objectives.

The rest of this paper is organized as follows. Section II introduces the background knowledge of this paper. Section III describes the motivations behind our proposal. Section IV is devoted to detail MP-DEA, including its basic algorithmic framework, the adopted MPRSS, and the analysis of the algorithm's computational complexity. Experimental settings and extensive experimental results together with their corresponding discussions are provided in Section V. Finally, Section VI draws the conclusions of the paper.

II. Background

A. Preliminaries: Basic Definitions

Generally, a MOP with only box constraints can be stated as follows [26]:

$$\begin{aligned} &\text{Minimize} \quad F(x) = (f_1(x), \ldots, f_M(x))^T \\ &\text{Subject to} \quad x \in \Omega \end{aligned} \tag{1}$$

where M is the number of objective functions, $\Omega = \prod_{i=1}^{n}[a_i, b_i] \subseteq \mathbb{R}^n$ is the decision (variable) space, $x = (x_1, \ldots, x_n)^T \in \Omega$ is a candidate solution. *F:* $\Omega \to \mathbb{R}^M$ is a vector of M conflicting objective functions, and $\mathbb{R}^M$ is called the objective space.

Definition 1. (Pareto dominance). x is said to dominate y, denoted as $x \prec y$ if and only if $f_i(x) \leq f_i(y)$ for every $i \in \{1, \ldots, M\}$ and $f_j(x) < f_j(y)$ for at least one index $j \in \{1, \ldots, M\}$.

Definition 2. (Pareto optimality). A solution x^* is Pareto-optimal if there is no other solution $x \in \Omega$ such that $x \prec x^*$.

Definition 3. (Pareto optimal set). The Pareto-optimal Set (PS) is the set of all Pareto-optimal solutions and it is defined as follows:

$$PS = \{x \in \Omega | x \text{ is Pareto optimal}\} \tag{2}$$

Definition 4. (Pareto optimal front). The Pareto-optimal front (PF) is the set of all Pareto-optimal solutions and it is defined as follows:

$$PF = \{F(x) \in \mathbb{R}^M | x \in PS\} \tag{3}$$

Definition 5. (Ideal point). The ideal point z^* is a vector $z^* = (z_1^*, z_2^*, \ldots, z_M^*)^T$, where z_i^* is the infimum of f_i for each $i \in \{1, 2, \ldots, M\}$.

Definition 6. (Nadir point). The nadir point z^{nad} is a vector $z^{nad} = (z_1^{nad}, z_2^{nad}, \ldots, z_M^{nad})^T$, where z_i^{nad} is the supremum of f_i over the PS for each $i \in \{1, 2, \ldots, M\}$.

Definition 7. (Reference point). A reference point RP is an M-dimensional vector $RP = (rp_1, rp_2, \ldots, rp_M)^T$ that satisfies the two following conditions:

$$rp_1 + rp_2 + \cdots + rp_M = 1 \tag{4}$$

$$rp_i \in \{0, \frac{1}{p}, \frac{2}{p}, \ldots, \frac{p}{p}\} \quad i = 1, \ldots, M \tag{5}$$

where p is a user-definable positive integer.

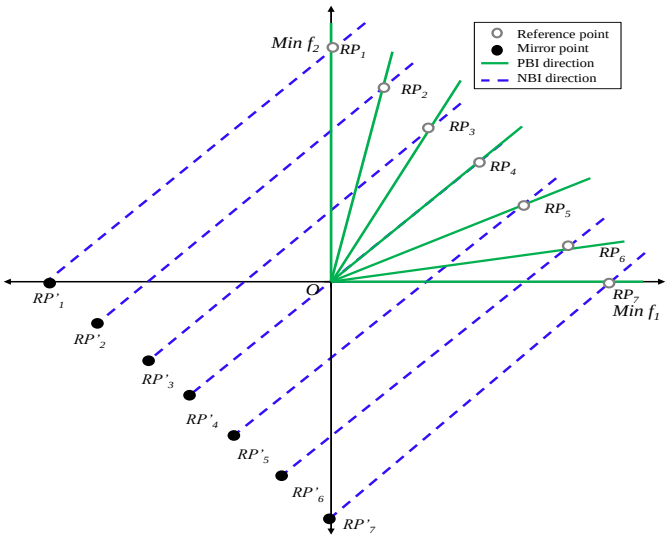

Fig. 1: Illustration of the reference point, mirror point, PBI direction, and NBI direction concepts.

Definition 8. (Mirror point). The M-dimensional vector $RP^{'} = (rp_1^{'}, rp_2^{'}, \ldots, rp_M^{'})^T$ is the mirror point of the reference point $RP = (rp_1, rp_2, \ldots, rp_M)^T$ if it satisfies the following condition:

$$rp_i^{'} = rp_i - 1 \quad i = \{1, 2, \ldots, M\} \tag{6}$$

Definition 9. (PBI direction). A PBI direction is a line passing through the origin to a reference point RP with a direction $\overrightarrow{ORP}$.

Definition 10. (Normal-Boundary Intersection (NBI) direction). A NBI direction is a line passing through a mirror point $RP^{'}$ to a reference point RP with a direction $\overrightarrow{RP^{'}RP}$.

Fig. 1 illustrates the decomposition concepts of Definitions 7-10.

B. Related Works

Recently, Ishibuchi et al. [9] have demonstrated that the performance of decomposition-based algorithms strongly depends on the shape of the PF. In fact, decomposition-based algorithms that use a predefined set of uniformly distributed reference points have shown good performance on problems with regular PFs. However, their performance deteriorates when solving problems that are characterized with: (1) degenerate, (2) discontinuous, (3) inverted, and (4) non-linear PFs, since most of the reference points may not have a solution along the PF. Moreover, the uniform distribution on a hyperplane does not translate into a uniform distribution on a non-linear PF [27].

In the literature, several works have been proposed to improve the performance of decomposition-based MaOEAs on problems with irregular PFs [27]. Qi et al. [28] proposed a new version of MOEA/D called MOEA/D-AWA to solve MOPs with complex PFs. The authors proposed a weight vector initialization method and an Adaptive Weight vector Adjustment (AWA) strategy that regulates the distribution

of the weight vectors periodically according to the current population. The main advantage of MOEA/D-AWA is that it can obtain good uniformity on problems that have a shape with a sharp peak and a low tail. Nevertheless, the performance of MOEA/D-AWA has been investigated only on degenerate problems. A-NSGA-III [29] is a modified version of NSGA-III. It identifies non-useful reference points and reallocates them based on the distribution and association of the solutions. A-NSGA-III outperforms NSGA-III on irregular problems, but this technique can often lead to a redundancy of some reference points. Liu et al. [30] introduced an adaptive region decomposition algorithm called MOEA/D-AM2M to solve degenerate problems. The authors proposed to adaptively adjust to the objective space by dynamic direction vectors design. An adaptive region decomposition and weight vectors design were employed to extract useful information from the evolving population. MOEA/D-AM2M shows better performance than MOEA/D. However, all the considered problems are degenerate. RVEA uses a scalarization approach, termed the Angle Penalized Distance (APD). This approach assesses convergence by calculating the distance between candidate solutions and the ideal point, while diversity is maintained by measuring the angle between the candidate solutions and the reference vectors. A reference vector regeneration strategy is also employed in order to enhance the performance of RVEA on irregular PFs. The main advantage of this approach is that the angle-based strategy is able to adapt the directions to deal with different scales of objectives. RVEA faces difficulties when handling problems with steep sections [27]. Xiang et al. [18] introduced the VaEA algorithm that uses a worse elimination selection to dynamically adjust the search directions. Moreover, it employs the maximum vector angle-first principle to maintain the uniformity of the solution set. The performance of VaEA has been investigated on the DTLZ1-4 and WFG test suites with up to fifteen objectives. The obtained results have shown that VaEA does not obtain the best performance on the DTLZ1-4 test problems. In PICEA-w [31], weights and the solutions are co-evolved during the search process. New weights are generated randomly at each generation. Moreover, the weight vectors with the highest contribution to non-dominated solutions are maintained. PICEA-w has shown a good performance on MaOPs with irregular PFs. However, the random generation of weight vectors may affect its performance on MaOPs with degenerate PFs. Asafuddoula et al. [27] proposed a generalized version of the DBEA (g-DBEA) algorithm. This algorithm uses a reference vector adaptation mechanism to solve problems with regular and irregular PFs. g-DBEA uses two sets of reference vectors, termed active and inactive sets. Based on the association and non-dominance information during the search process, new reference vectors are generated and some reference points are removed to the inactive set. g-DBEA shows its effectiveness on MaOPs with regular and irregular PFs. However, the effect of the learning period (i.e., the τ parameter) requires further investigation. CA-MOEA [32] is a clustering-based algorithm that selects individuals according to a set of cluster centers in the last non-dominated front. CA-MOEA has proven his strength on problems with regular and irregular PFs, but the employed clustering-based adaptation may slow down the convergence in the early stage of the search. Besides, the performance of CA-MOEA needs to be investigated on MaOPs. CLIA [33] is a reference vector-based MaOEA that adopts an incremental learning of the PF via component interactions. It uses two interacting processes that are the cascade clustering and the reference point incremental learning. The first process guides the evolution of the individuals using the reference vectors of the second process, while the second process is employed to generate reference vectors using the feedback from the selection operator. MOEA/D-TPN [34] is an improved version of MOEA/D that handles MaOPs with complex PFs. A two-phase strategy that divides the optimization process into two phases and a niche-guided strategy that increases the population diversity are employed. The main limitation of this algorithm is that it employs some parameters that it is not easy for users to set in advance without any knowledge about the problem and that may vary with the difficulty of the considered problem. MOEA/D–LTD [35] traces the PF shape, in which the learning module predicts the PF shape and the decomposition function is adaptively adjusted to fit the PF shape. It proposes to use Gaussian process to fit the current PF.

III. Motivations

In spite of the popularity of decomposition-based algorithms in solving MaOPs, they face many challenges that considerably affect their performance. First, one of the main issues when using a pre-defined set of reference points is how to maintain the uniformity of the intersection points between the search directions and the PF. In fact, when facing a problem with complex PF (e.g., discontinuous and degenerate fronts) some reference directions cannot intersect the PF. Thus, generating a set of reference points/weight vectors beforehand cannot guarantee the uniformity of the approximated PF [18]. Second, the adaptation of the reference points is a challenging task for the following reasons. It is difficult to identify the timing and frequency to invoke the adaptive strategy. In fact, at the early stages of the search process, there may exist some inactive reference points (i.e., reference points with no solutions associated to them). If the adaptation is too frequent, the solutions may require a long traversal to reach the PF, while if it is not frequent, the reference points may not conform with the shape of the PF within an adequate computational budget [36]. Third, the generation of new reference points requires additional parameters and there is no ideal strategy to add/delete the reference points [27]. Finally, most existing decomposition-based algorithms employ the PBI scalarizing function in order to compare pairs of solutions. Nevertheless, the PBI scalarizing function employs the penalty parameter θ. Mohammadi et al. [20] have shown that there is no unique θ value that works well on problems that have different PF characteristics with a different number of objectives.

In general, decomposition-based algorithms that use PBI directions are well-suited to solve MaOPs with regular PFs. Fig. 2 (a) gives an example where a set of uniformly distributed reference points (i.e., a set of PBI directions) corre-

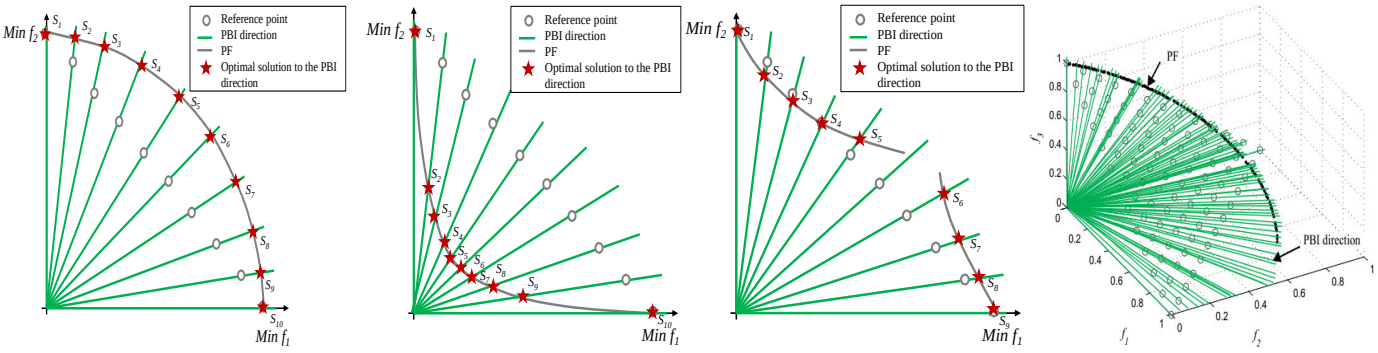

(a) Concave PF (b) Strongly Convex PF (c) Disconnected, convex PF (d) Degenerate PF

Fig. 2: An example illustrating that using the PBI directions may lead to a distribution of optimal solutions that depends on the shape of the PF.

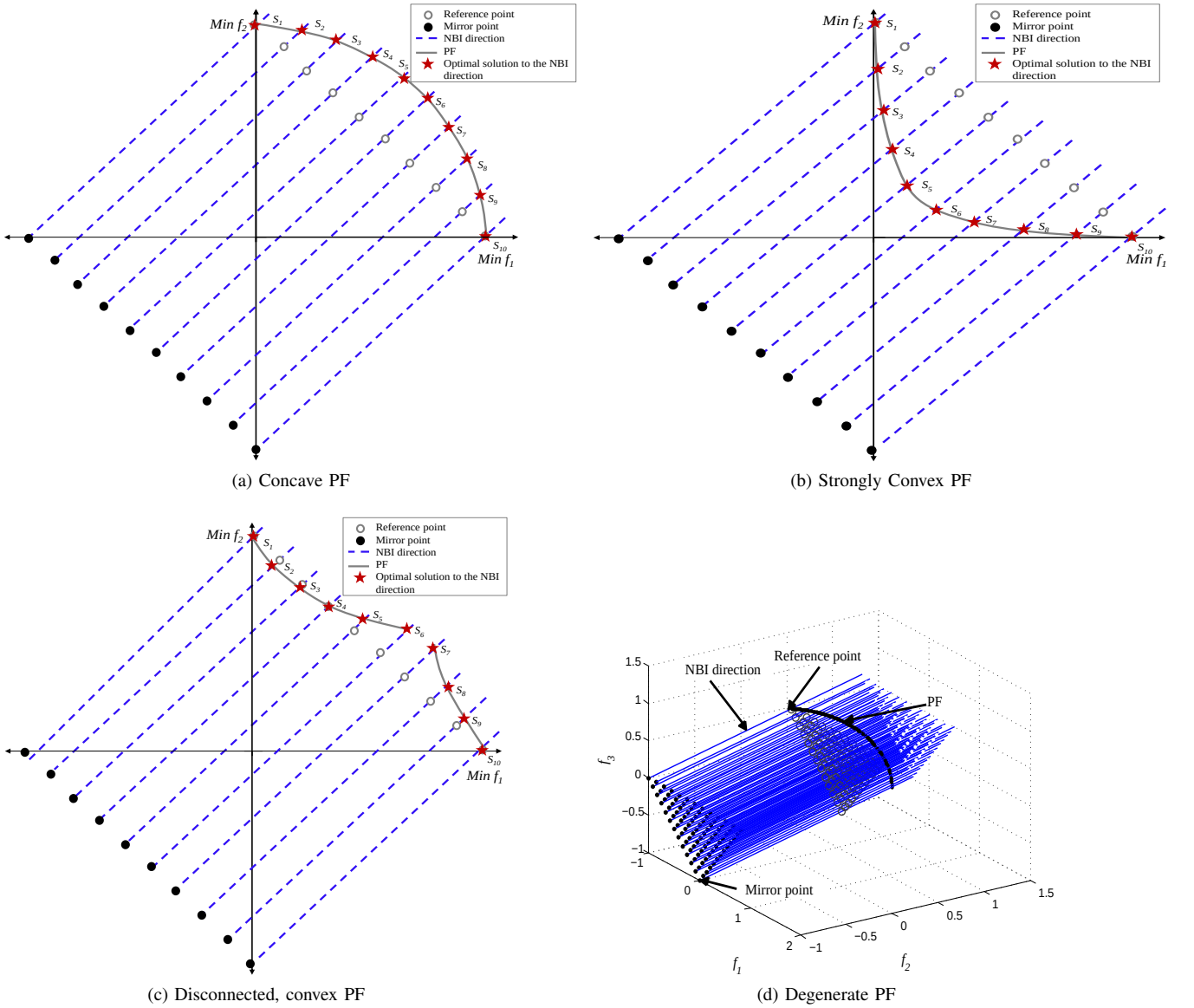

(a) Concave PF (b) Strongly Convex PF

(c) Disconnected, convex PF (d) Degenerate PF

Fig. 3: An example illustrating that using pre-defined sets of uniformly distributed reference points and mirror points (i.e., NBI directions) guarantee a uniformly distribution of the optimal solutions.

spond to a set of uniformly distributed optimal solutions. However, when the shape of the PF is irregular, decomposition-based algorithms appear to struggle due to the inconsistency between the shape of the PF and the distribution of the PBI directions. Figs. 2 (b)-(d) show three examples where a set of optimal solutions are obtained by a set of PBI directions. In Fig. 2 (b), one can notice that the distances between (S_1, S_2) and (S_9, S_{10}) are larger than the distances between the other adjacent solutions. Figs. 2 (c) and (d) show that the solutions are not uniformly distributed along the PF and some parts of the PF do not have intersection points with the PBI directions. These observations demonstrate the difficulties encountered when using the PBI directions, specifically when solving real world problems where the information about their PFs is unknown.

The NBI method [37] has been widely employed to find a uniformly spread Pareto optimal solutions using a set of NBI directions that are able to cover the PF regardless of its geometry. Figs. 3 (a)-(d) illustrate that the equidistant NBI directions lead to a uniformly distribution of the solutions on concave, convex, disconnected, and degenerate PFs.

The previously described problems of the PBI method are precisely the underlying motivations of our work. In this paper, we propose a new decomposition-based approach that combines the PBI and the NBI directions in order to use their strength. Hence, solutions associated to the same subregion are compared based on the acute angle and the Euclidean distance metrics. The acute angle metric is a PBI direction-based metric that measures diversity and in some cases convergence, while the Euclidean distance metric is a NBI direction-based metric that measures the convergence and the uniformity.

Since some reference points may have no intersection in the case of discontinuous and/or degenerate PF, we suggest to not remove the inactive reference points, but to ask the Decision Maker (DM) to interact with the algorithm by increasing the number of reference points after a number of generations. We simply add a set of reference points centering around the crowded reference points [29]. This strategy guarantees the uniformity, since it increases the number of points intersecting the PF. It is described in Appendix A. In the next section, we describe our proposed MPR and MP-DEA algorithm.

IV. The Proposed Algorithm: MP-DEA

In this section, we first describe the general framework of MP-DEA. Thereafter, we detail its different components. Finally, we present the MPR and the complexity of MP-DEA.

A. General Framework and Pseudocode

Fig. 4 provides the overall framework of MP-DEA. The pseudocode of MP-DEA can be described in Algorithm 1 and Algorithm 2. First, an $RPSet$ of W reference points is generated using Das and Dennis's systematic approach [37] (line 3 of Algorithm 1). Then, a set of mirror points $MSet$ is generated so that each reference point in $RPSet$ has its mirror point in $MSet$ (line 4 of Algorithm 1). After that, a population with N individuals is randomly generated (line 5 of Algorithm 1). Next, we initialize the ideal point

Algorithm 1 MP-DEA pseudocode

Input: Number of objectives *M*, number of divisions p, population size *N*, maximum number of generations G_{max}, generations of DM interactions tab_{inter}
Output: Population P_{t+1}
01: **Begin**
02: $t \leftarrow 0$;
03: $RPSet \leftarrow$ generate_reference_points (M, p);
04: $MSet \leftarrow$ generate_mirror_points $(RPSet)$;
05: $P_0 \leftarrow$ generate_initial_population (N);
06: $z^* \leftarrow$ initialize_ideal_point (P_0);
07: $z^{nad} \leftarrow$ initialize_nadir_point (P_0);
08: **While** $(t < G_{max})$ **do**
09: **If** $((t \in tab_{inter})$ and (DM_decision = 0)) */* DM_decision is set to 0 if the DM decides to interact; otherwise, it is set to 1 */*
10: $RPSet \leftarrow$ update_reference_points $(RPSet)$; */* The update of the reference points is performed using the method described in Appendix A */*
11: $MSet \leftarrow$ update_mirror_points $(RPSet)$;
12: **End If**
13: $P_{t+1} \leftarrow$ MP-DEA_basic_iteration $(P_t, N, RPSet, MSet, z^*, z^{nad})$;
14: $t \leftarrow t + 1$;
15: **End While**
16: **Return** P_{t+1}
17: **End**

Algorithm 2 MP-DEA_basic_iteration pseudocode

Input: Current population P_t, population size *N*, reference point set $RPSet$, mirror point set $MSet$, z^* ideal point, , z^{nad} nadir point
Output: Population P_{t+1}
01: **Begin**
02: $Q_t \leftarrow$ create_offspring_population (P_t);
03: $R_t \leftarrow$ create_union_population (P_t, Q_t);
04: $S_t \leftarrow$ non_dominated_sorting (R_t);
05: $z^* \leftarrow$ update_ideal_point (S_t);
06: $S_t \leftarrow$ normalize (S_t, z^*, z^{nad});
07: $S_t \leftarrow$ associate_population_members $(S_t, RPSet)$;
08: $S_t^{'} \leftarrow$ non_MPR-dominated_sorting $(S_t, RPSet, MSet)$;
09: $P_{t+1} \leftarrow \emptyset$;
10: $i \leftarrow 1$;
11: **While** ((size (P_{t+1}) + size $(S_t^{'}(i))) < N$) **do** */* $S_t^{'}(i)$ is the i^{th} front of the ranked population $S_t^{'}$ */*
12: $P_{t+1} \leftarrow P_{t+1} \cup S_t^{'}(i)$;
13: $i \leftarrow i + 1$;
14: **End While**
15: **For** $j = 1$ to (N - size (P_{t+1})) **do**
16: $P_{t+1} \leftarrow$random_select_individual $(j, S_t^{'}(i))$;
17: **End For**
18: **Return** P_{t+1}
19: **End**

z^* with the minimum value found so far for each objective f_i in P_0, since it is time consuming to compute the exact z_i^* (line 6 of Algorithm 1). The Nadir point z^{nad} is also initialized with the maximum value found so far for each objective f_i in Step 7 of Algorithm 1. Steps 8-15 of Algorithm 1 are executed while the number of generations does not exceed G_{max}. Steps 9-12 are executed only if the process of interacting with the DM is reached and the DM decides to perform an interaction. In this case, we increase the number of reference points (line 10 of Algorithm 1) and the number of mirror points (line 11 of Algorithm 1). The mirror points are updated by generating a set of mirror points that correspond to the new set of reference points. In Step 13 of Algorithm 1, the MP-DEA_basic_iteration procedure is performed, whose pseudocode is given in Algorithm 2. The MP-DEA_basic_iteration procedure can be described as follows. An offspring population Q_t is created by using the

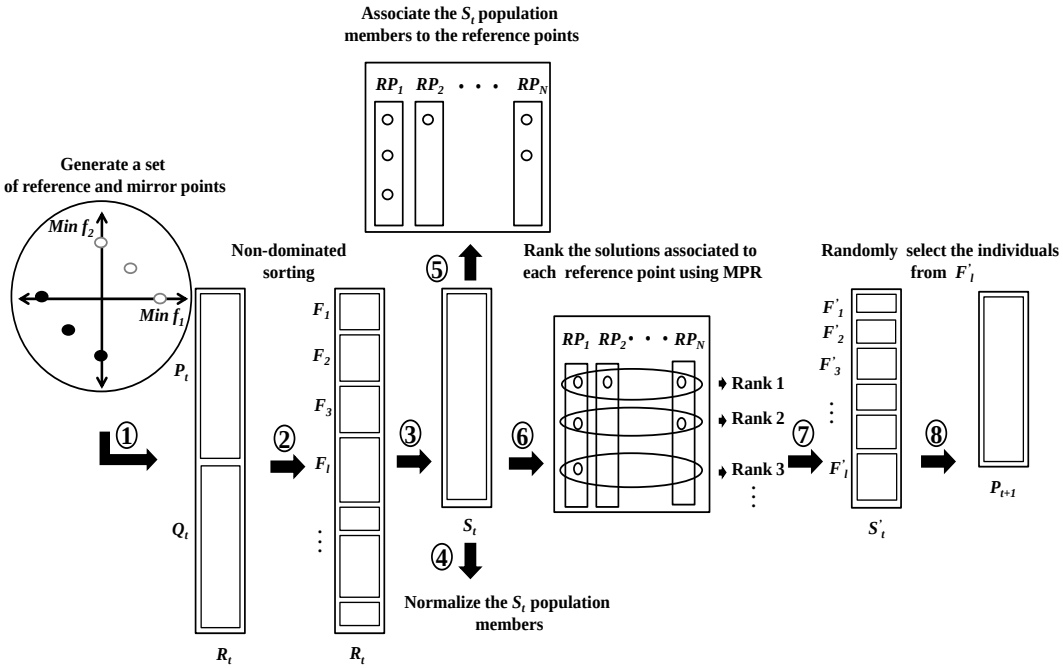

Fig. 4: Overall framework of the MP-DEA algorithm.

recombination operator (line 2 of Algorithm 2). Next, P_t and Q_t are merged together to form the union population R_t with $2N$ individuals (line 3 of Algorithm 2). In line 4 of Algorithm 2, we perform the non-dominated sorting to classify the population R_t into several fronts and a population S_t formed with the best Pareto non-domination levels is created. The population $S_t = \cup_{i=1}^{\tau} F_i$, where F_i is the i^{th} Pareto non-dominated front of the population R_t and τ satisfies $\sum_{i=1}^{\tau-1}|F_i| < N$ and $\sum_{i=1}^{\tau}|F_i| \geq N$. We then update the ideal point z^* using the population S_t (lines 5 of Algorithm 2). Thereafter, we normalize the S_t population members (line 6 of Algorithm 2). We note that the nadir point z^{nad} is updated in the normalization procedure. After performing the normalization, we associate the members in S_t to the reference points in $RPSet$ (line 7 of Algorithm 2). After that, a non-dominated sorting based on MPR is performed to form a new population $S_t^{'}$ classified into different MPR non-domination levels $(F_1^{'}, F_2^{'}, etc)$ (line 8 of Algorithm 2). Once the $S_t^{'}$ population is constructed, we fill the population P_{t+1} using the MPR non-domination levels (lines 11-14 of Algorithm 2). However, similarly to θ-DEA, we randomly select the individuals from the last accepted front $F_l^{'}$ (lines 15-17 of Algorithm 2).

B. Reference and Mirror Points Generation Methods

The generation of the reference points in MP-DEA is done using Das and Dennis's systematic approach [37]. The number of reference points depends on the number of objectives M and the number of divisions considered along each objective axis p. The number of reference points is calculated using the following equation [38]:

$$W = \binom{M+p-1}{p} \tag{7}$$

If $p < M$ there are no intermediate reference points that are created using this method. In order to generate intermediate reference points within the simplex, we should set $M \geq p$. For the sake of diversity and computational cost, we use a two-layer reference point generation method as suggested in [13]. Thus, the number of reference points can be expressed as follows [13]:

$$W = \binom{M+p_1-1}{p_1} + \binom{M+p_2-1}{p_2} \tag{8}$$

where p_1 and p_2 represent the divisions of boundary and inside layers, respectively.

After the generation of the $RPSet$, we then create the $MSet$ of W mirror points by decreasing the coordinates of the reference points by 1. Note that there is no one unique method to generate the mirror points. In this paper, we have employed the simplest one. Fig. 5 illustrates the two-layer reference and mirror points generation methods.

C. Creation of the Offspring Population

In MaOPs, the usual recombination operator may be less effective in producing offspring solutions that are close to their parents. In order to address this issue, we propose to use the same special recombination scheme employed in NSGA-III and θ-DEA, since our algorithm is inspired by the two above algorithms. This approach consists in using a large distribution index for the Simulated Binary Crossover (SBX) operator [39]. The recombination operator starts by randomly selecting two parent solutions from the current population P_t. Then, a child solution is created by applying the SBX operator with a large distribution index and polynomial-based mutation [40].

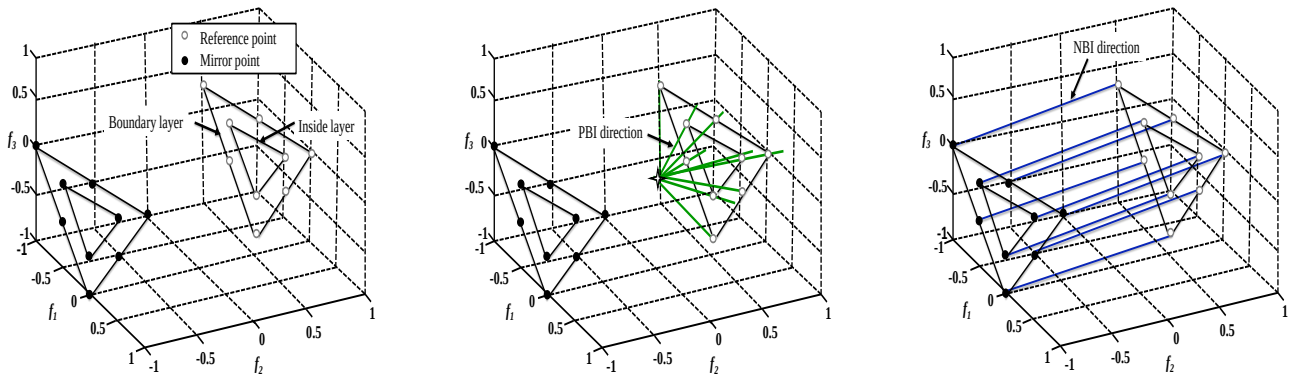

(a) Two-layer reference and mirror points generation methods (b) PBI directions (c) NBI directions

Fig. 5: Illustration of the reference and mirror points generation methods.

D. Normalization Procedure

After the creation of the S_t population, we normalize the objective values of its individuals. This step is important when solving problems characterized by PFs whose objective values are badly scaled. Thus, the objective $f_i(x)$, $i = 1, 2, \ldots, M$, is normalized as follows:

$$\tilde{f}_i(x) = \frac{f_i(x) - z_i^*}{z_i^{nad} - z_i^*} \tag{9}$$

where z_i^* is estimated by the best value found so far for objective f_i. However, the estimation of z_i^{nad} is similar to that in θ-DEA. We first start by identifying the extreme point E_j in the objective axis f_j. Thus, we have to find the solution $x \in S_t$ that minimizes the following Achievement Scalarizing Function (ASF) [38]:

$$ASF(x, a_j) = \max_{i=1}^{M} \left\{ \frac{1}{a_j} \left| \frac{f_i(x) - z_i^*}{z_i^{nad} - z_i^*} \right| \right\} \tag{10}$$

where $a_j = (a_{j,1}, a_{j,2}, \ldots, a_{j,M})^T$ is the axis direction of the objective axis f_j. We note that $a_{j,i} = 10^{-6}$ if $i \neq j$ and $a_{j,i} = 1$, otherwise. The extreme point E_j is assigned the objective vector of the solution x that minimizes the above described ASF (i.e., $E_j = x$). After finding the M extreme points for all the objectives, we construct an M-dimensional linear hyperplane. Let the matrix $D = (E_1 - z^*, E_2 - z^*, \ldots, E_M - z^*)^T$ and $u = (1, 1, \ldots, 1)^T$, the intercepts are calculated using the following equation [38]:

$$\begin{pmatrix} (c_1 - z_1^*) \\ (c_2 - z_2^*) \\ \ldots \\ (c_M - z_M^*) \end{pmatrix} = D^{-1}u \tag{11}$$

where $c_1, c_2, \ldots, c_M$ represent the intercepts of the hyperplane with the directions $(1, z_2^*, \ldots, z_M^*)^T$, $(z_1^*, 1, \ldots, z_M^*)^T, \ldots,$ $(z_1^*, z_2^*, \ldots, 1)^T$, respectively. Finally, the value of z_i^{nad} is set as c_i. For more details of the hyperplane construction and the intercepts formation, please refer to [38].

E. Association Procedure

The association procedure of MP-DEA is performed in the normalized objective space, where the ideal point z^* is the origin. At each generation, the individuals of the S_t population are associated to the reference points in the $RPSet$. For the association operator, the norm of each solution in S_t is computed. The norm of a solution x is defined as shown below [18]:

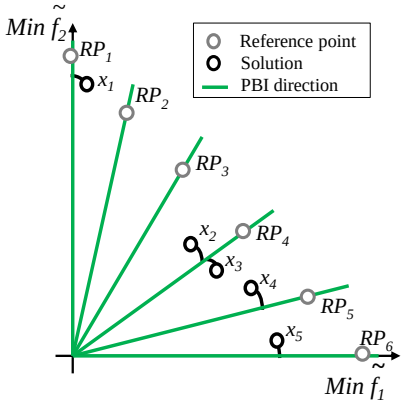

Fig. 6: Illustration of the association operation using acute angle.

$$norm(x) \triangleq \sqrt{\sum_{i=1}^{M} \tilde{f}_i(x)^2} \tag{12}$$

The norm is used to calculate vector angles between a solution and a reference point. The vector (acute) angle between a solution x and a reference point RP_j is defined as follows:

$$angle(x, RP_j) \triangleq \arccos \left| \frac{\tilde{F}(x) \bullet RP_j}{norm(x).norm(RP_j)} \right| \tag{13}$$

where $\tilde{F}(x) = (\tilde{f}_1(x), \tilde{f}_2(x), \ldots, \tilde{f}_M(x))^T$, $RP_j = (rp_{j1}, rp_{j2}, \ldots, rp_{jM})^T$, $\tilde{F}(x) \bullet RP_j$ returns the inner product between $\tilde{F}(x)$ and RP_j, and it is defined as follows:

$$\tilde{F}(x) \bullet RP_j = \sum_{i=1}^{M} \tilde{f}_i(x).rp_{ji} \tag{14}$$

It is worth mentioning that using this association procedure each solution will be assigned to its closest reference point in

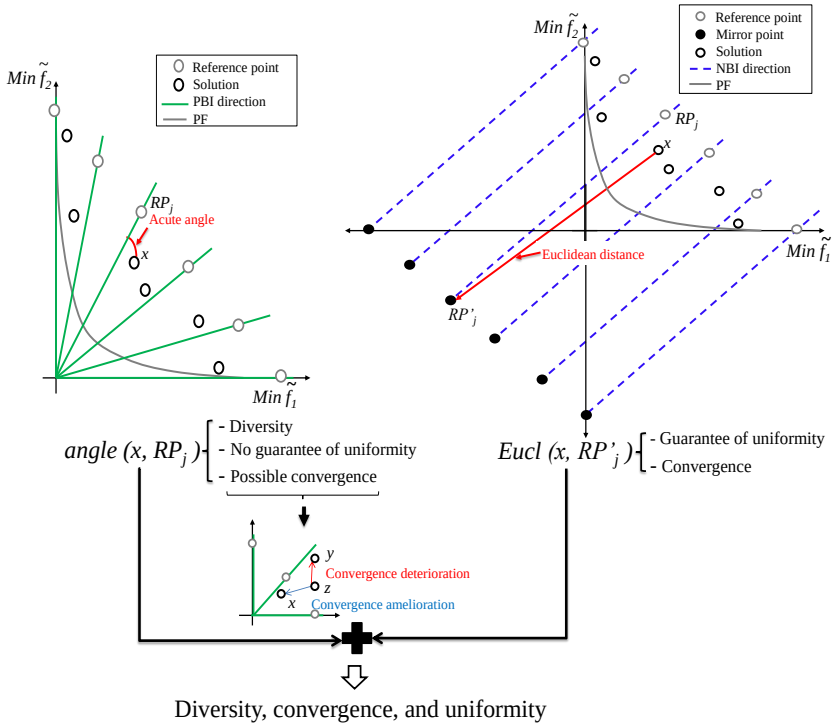

Fig. 7: Illustration of the angle and Euclidean distance metrics.

the normalized objective space. Fig. 6 illustrates the association operation in a two-dimensional objective space. According to the vector angle, x_1 is associated to RP_1, both x_2 and x_3 are associated to RP_4, x_4 is associated to RP_5, and x_5 is associated to RP_6.

F. MPR-based Selection Strategy (MPRSS)

The proposed MPR is defined on the population S_t. After the association of the solutions to the reference points, we use the MPR to sort the solutions associated to the same reference point.

Definition 11. (Mirror Point-based Relation (MPR)). Given two solutions x and $y \in S_t$ and associated to the same reference point RP_j, x is preferred to y iff:
$angle(x, RP_j) + Eucl(x, RP'_j) < angle(y, RP_j) + Eucl(y, RP'_j)$

where $j \in \{1, 2, \ldots, W\}$, RP'_j is the mirror point assigned to x, $angle(x, RP_j)$ is the acute angle between the solution x and the reference point RP_j, and $Eucl(x, RP'_j)$ is the Euclidean distance between the solution x and the mirror point RP'_j. Before evaluating the solutions, we perform a normalization of the angle values and the Euclidean distances so that they have the same range by identifying the minimum and maximum angle values and Euclidean distances found so far in the population S_t. Fig. 7 illustrates the angle and Euclidean distance metrics of the MPR. The angle metric measures diversity and in some cases convergence, while the Euclidean distance metric measures uniformity and convergence. The MPR states that when x is better than y in terms of diversity, convergence, and uniformity, x is preferred over y. Hence, the solutions are compared using the PBI (acute angle) and the NBI (Euclidean distance) metrics. In addition, the combination of the acute angle value and the Euclidean distance makes this relation able to control the balance between diversity, convergence, and uniformity without using a penalty parameter. Fig. 8 illustrates the execution of the MPRSS environmental selection on a population containing ten individuals and six subregions (i.e., six reference points). Fig. 8 (a) shows the execution of the non-MPR-dominated sorting. One can notice that using our non-MPR-dominated sorting the solutions with the same order have the same rank. One can notice from Fig. 8 (a) that the solution x_2 is preferred to x_3 using MPR, since x_2 has lower acute angle and Euclidean distance values. After executing the MPR, we adapt the fast non-dominated sorting [7] by partitioning the S_t population into different MPR non-domination levels. Fig. 8 (b) highlights the third region and shows the directions that are employed in the comparison of the solutions.

G. Computational Complexity Analysis

The basic framework of MP-DEA remains similar to θ-DEA. Hence, we can follow the same principle used in [38] to compute the complexity of MP-DEA. The computational cost of a generation of MP-DEA can be detailed as follows. The initialization procedures of z^* and z^{nad} require $O(N)$ computations (lines 6 and 7 in Algorithm 1). The update of the reference points requires $O(N)$ computations (line 10 in Algorithm 1). The non-dominated sorting (line 4 in Algorithm 2) of the population R_t with $2N$ individuals having M-dimensional objective vectors requires $O(MN^2)$ computations. The normalization of the S_t population with $2N$ solutions having M objectives requires $O(MN)$ (line 6

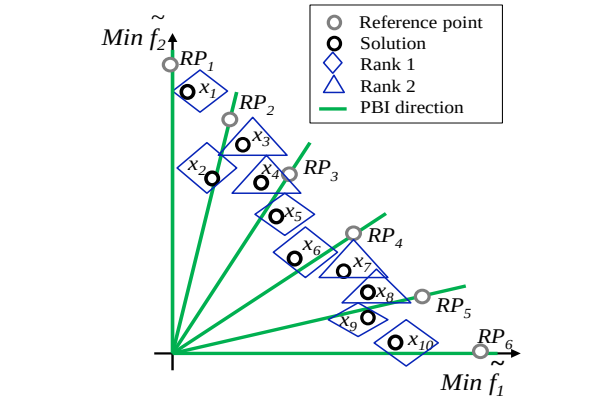

(a) MPRSS environmental selection

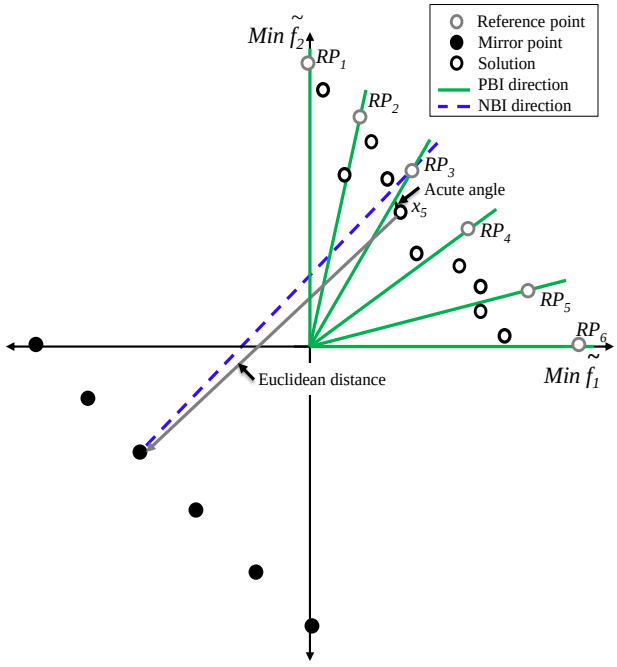

(b) Illustration of the acute angle and Euclidean distance

Fig. 8: An illustration of the execution of the MPRSS environmental selection.

in Algorithm 2). In order to associate the solutions, we have to compute the W acute angle values for each solution in S_t and each one of them is computed in $O(M)$ computations. Thus, the association procedure requires $O(MN^2)$ computations, since $W \simeq N$ in our simulations (line 7 in Algorithm 2). The non-MPR-dominated sorting of the S_t population having M objectives also needs $O(MN^2)$ computations in the worst case (line 8 in Algorithm 2). Similarly to θ-DEA, the overall complexity of one generation of MP-DEA is approximately equal to $O(MN^2)$.

V. Experimental Study

This section is structured as follows. First, we present the test problems, the performance measures, and the statistical testing that are used in our experiments. Second, we introduce the algorithms under comparison and we provide the experimental settings adopted in this paper. Finally, we discuss the obtained results.

TABLE I: Properties of the test problems [38], [9], [25].

Problem	Properties
Regular PF	
DTLZ1	Linear, Multi-modal
DTLZ2	Concave
DTLZ3	Concave, Multi-modal
DTLZ4	Concave, Biased
WFG4	Concave, Multi-modal, Scaled
WFG5	Concave, Deceptive, Scaled
WFG6	Concave, Non-separable, Scaled
WFG7	Concave, Biased, Scaled
WFG8	Concave, Biased, Non-separable, Scaled
WFG9	Concave, Biased, Multi-modal, Deceptive, Non-separable, Scaled
Irregular PF	
WFG1	Mixed, Biased, Scaled
WFG2	Convex, Disconnected, Multi-modal, Non-separable, Scaled
WFG3	Linear, Degenerate, Non-separable, Scaled
DTLZ1^{-1}	Rotated
DTLZ2^{-1}	Convex
DTLZ3^{-1}	Convex
DTLZ4^{-1}	Convex
MaF4	Concave, Multi-modal, Badly-scaled, No single optimal solution in any subset of objectives
MaF5	Convex, Biased, Badly-scaled
MaF6	Concave, Degenerate
MaF7	Mixed, disconnected, Multi-modal
MaF9	Linear, Degenerate
MaF12	Concave, Non-separable, Biased Deceptive

A. Test Problems

For the purposes of our comparison, four test problems from the well-known DTLZ test suite (DTLZ1-4) [23], four inverted (DTLZ1-4) test problems [9], nine WFG test problems (WFG1-9) [24], and six MaF benchmark problems (MaF4-7, MaF9, and MaF12) [25] have been employed to conduct our experiments. In our experimental study, we considered instances having $M \in \{3, 5, 8, 10, 15\}$ objectives.

For the DTLZ, inverted DTLZ, and MaF4-7 test instances, the number of decision variables is set to $n = M + r - 1$, where $r = 5$ for DTLZ1 and DTLZ^{-1}, $r = 10$ for DTLZ2-4, DTLZ2-4^{-1}, MaF4-6, and MaF12, while $r = 20$ for MaF7. The number of decision variables is set to $n = 2$ for MaF9. According to the recommendations in [24], the number of decision variables is set to $n = k + l$ for the WFG test problems, where the position-related variable $k = 2 \times (M-1)$, and the distance-related variable $l = 20$. The PFs of the above test suites have different characteristics and they present a significant challenge for an algorithm to find a well-converged and well-distributed solution set. The main properties of all test instances are summarized in Table I.

B. Performance Measures

We adopted the Inverted Generational Distance (IGD) [41] and the HyperVolume (HV) [42] to assess the performance of each algorithm. The IGD and HV provide complementary information about convergence and diversity. Let F^* be a set

of uniformly distributed points over the PF and S, the obtained solution set.

- **IGD:** The IGD indicator assesses both convergence and diversity. This indicator computes the average Euclidean distance from each solution composing the PF to its closest solution in S. The IGD indicator is defined as follows [41]:

$$IGD(S) = \frac{\sum_{x^* \in F^*} dist(x^*, S)}{|F^*|} \quad (15)$$

  where $dist(x^*, S)$ is the Euclidean distance between a point $x^* \in F^*$ and its nearest solution in S. A smaller value of the IGD is better.
- **HV:** This indicator measures the volume of the objective space between S and a specified reference point z^r. The HV indicator can be defined as follows [13]:

$$HV(S) = VOL(\cup_{x \in S}[f_1(x), z_1^r] \times [f_M(x), z_M^r]) \quad (16)$$

  where $VOL(\Delta)$ indicates the Lebesgue measure. A larger value of the HV indicator is better. In this study, we first normalize the solutions using the ideal point and the nadir point of the PF. Then, the HV is calculated using the reference point $(1.1, 1.1, \ldots, 1.1)^T$ [9], [38]. The HV is calculated using the WFG algorithm [43] when $M < 10$ and a Monte Carlo simulation [44] when $M \geq 10$.

In the calculation of the IGD metric, a set of Pareto-optimal solutions is required. For DTLZ1-4, we use the same method reported in [13] to form the reference Pareto-optimal points. This method is able to identify the intersecting points between the set of reference points generated using Das and Dennis's systematic approach and the Pareto-optimal surface of the DTLZ1-4 test problems, since the exact Pareto-optimal surfaces of the above test problems are known. The number of reference points for calculating the above described performance measures should be large enough so as to cover the PF. Thus, we use a larger number of divisions in the reference points' generation method. For DTLZ1-4^{-1}, the reference PF is obtained by scaling the points of the DTLZ problems.

For the WFG test problems, we use the same methods employed in [18] to generate the reference Pareto-optimal points. The range of the i^{th} objective of the WFG problems is $[0, 2i]$, where $(i = 1, 2, 3, \ldots, M)$. Moreover, the PF of WFG4-9 is a hypersphere. Thus, we generate the reference Pareto-optimal points of WFG4-9 by multiplying the i^{th} objective of the reference points of DTLZ2-4 by $2i$. Therefore, the number of reference points is the same as in the DTLZ test problems. For WFG1-2, their PFs are irregular. Thus, we sample a large number of points in the underlying space $[0, 1]^{M-1}$ and then we calculate the objective values according to analytical expressions of the shape functions. After that, we remove all dominated points to constitute the final reference set. For WFG3, it was originally designed to have a degenerate PF but for more than three objectives it also has a non-degenerated PF. Thus, we constructed the reference point set by selecting all the non-dominated solutions from all the returned solutions obtained from 31 independent runs of each algorithm.

The reference PFs for MaF4-7, MaF9, and MaF12 problems are generated using the open source software jMetal [45].

TABLE II: Settings of the number of divisions and population size for different numbers of objectives.

M	Divisions (p)	MP-DEA VaEA RVEA θ-DEA	MOEA/D-AWA MOEA/DD
3	12	92	91
5	6	212	210
8	3, 2	156	156
10	3, 2	276	275
15	2, 1	136	135

C. Statistical Testing

In this experimental study, the Wilcoxon rank sum test [46] was applied in a pairwise fashion at a 0.05 significance level to evaluate the statistical significance of the obtained results. This is a statistical test that is used to compare the performance of two stochastic algorithms. In fact, it is important to use statistical tests, since each algorithm can behave differently using the same input parameters from one run to another. In our study, we performed 31 runs for each pair (algorithm, problem) to facilitate the median extraction. The results of the Wilcoxon rank sum test are presented in the form of (-: no significance) and (+: significance).

D. Algorithms under Comparison

In this study, we compare MP-DEA with respect to five decomposition-based algorithms which are: VaEA [18], RVEA [47], MOEA/D-AWA [28], θ-DEA [38], and MOEA/DD [13]. In the following, we summarize the working principles of the considered peer algorithms.

- **VaEA [18]:** VaEA is a vector angle-based algorithm. It uses the maximum-vector-angle-first principle to maintain the diversity, while the convergence is maintained using the worst elimination principle.
- **RVEA [47]:** RVEA uses an angle penalized distance to balance convergence and diversity. An adaptation strategy is employed to dynamically adjust the distribution of the reference vectors.
- **MOEA/D-AWA [28]:** MOEA/D-AWA employs an adaptive weight vector adjustment strategy to solve MOPs with complex PFs.
- **θ-DEA [38]:** θ-DEA uses a θ-dominance, which is based on the PBI scalarizing function. The θ-dominance has the ability to maintain the balance between convergence and diversity.
- **MOEA/DD [13]:** MOEA/DD combines dominance and decomposition to achieve a balance between convergence and diversity. It uses niching scenarios to preserve solutions associated to isolated subregions.

E. Experimental Settings

The parameters settings of the considered algorithms in this study can be summarized as follows:

1) **Parameters settings for operators:** The SBX and polynomial-based mutation operators were used to perform the variation. The crossover probability p_c was set

TABLE III: Settings of *MFE* for different test instances.

Problem \ M	3	5	8	10	15
DTLZ1 DTLZ1^{-1}	36800	127200	117000	276000	204000
DTLZ2 DTLZ2^{-1}	23000	74200	78000	207000	136000
DTLZ3 DTLZ3^{-1}	92000	212000	156000	414000	272000
DTLZ4 DTLZ4^{-1}	55200	212000	195000	552000	408000
WFG1-9	-	159000	-	552000	408000
MaF4-6	-	140000	-	190000	240000
MaF7	-	240000	-	290000	340000
MaF9	-	100000	-	100000	100000
MaF12	-	140000	-	190000	240000

TABLE IV: Settings of the DM's interactions for different test problems with discontinuous and degenerate PFs.

Problem \ M	3	5	8	10	15
WFG2	-	127200	-	276000 414000	136000 238000 306000
WFG3	-	127200	-	276000 414000	136000 238000 306000
MaF6	-	95400	-	96600 138000	102000 136000 170000
MaF7	-	169600	-	124200 207000	170000 238000 272000
MaF9	-	74200	-	41400 69000	34000 61200 81600

to 1.0, while the mutation probability p_m was set to $1/n$, where n is the number of variables in the decision space. For the SBX operator, the distribution index η_c was set to 30 except for MOEA/D-AWA, for which it was set to 20 and the distribution index of the mutation operator η_m was set to 20.

2) **Population size:** The population size N of MP-DEA, VaEA, RVEA, and θ-DEA was set as in [29]. For MOEA/DD and MOEA/D-AWA, the population size was set as in MOEA/D. Table II summarizes the value of N for different numbers of objectives.
3) **Stopping condition:** The stopping condition of an algorithm is the Maximum number of Function Evaluations (*MFE*). Table III shows the settings of *MFE* for different number of objectives. For MP-DEA the maximum number of generations (termination condition) can be easily determined by $G_{max} = MFE/N$.
4) **DM interactions:** The DM may needs to interact after performing a number of function evaluations . Table IV shows the function evaluations in which the DM decides whether he increments the number of reference or not.
5) **Specific parameters settings:** For RVEA, the index α which is adopted to control the rate of change of the penalty function was set to 2 and the frequency f_r was set to 0.1. For MOEA/DD, the neighborhood size T was set to 20, the penalty parameter θ was set to 5 and the neighborhood selection probability δ was set to 0.9. FOR θ-DEA the penalty parameter θ in PBI was set to 5. In MOEA/D-AWA, the maximal number of adjusting subproblems was set as $0.05N$, the computational resources for the weight adaptation was set as 0.8, and the size of the external elite was set as $1.5N$.

F. Results and Discussion

In this section, we describe the obtained experimental results to validate the performance and the effectiveness of MP-DEA. The conducted experiments can be divided into three parts based on the employed test suite.

1) Performance Comparisons on the DTLZ Test Suite: In this category, we consider four problems: DTLZ1, DTLZ2, DTLZ3, and DTLZ4. Table V presents the median IGD and HV values obtained by MP-DEA, VaEA, RVEA, MOEA/D-AWA, θ-DEA, and MOEA/DD on the DTLZ1-4 test problems. MP-DEA shows a clear advantage over its competitors on the majority of the test instances.

For DTLZ1, MP-DEA clearly outperforms VaEA, RVEA, MOEA/D-AWA, and θ-DEA in all three- to fifteen-objective problem instances. MOEA/DD performs better than MP-DEA in three- and five-objective cases.

For DTLZ2, both MP-DEA and VaEA have a similar performance in terms of IGD, while MP-DEA has the best performance in terms of HV as it wins in almost all problem instances except for the eight-objective case. θ-DEA obtains the best median IGD value on the five-objective case.

For DTLZ3, MP-DEA has the best performance in terms of IGD and HV. VaEA and RVEA have a similar performance, while MOEA/DD have the worst performance.

MOEA/D-AWA performs significantly worse than MP-DEA, VaEA, RVEA, and θ-DEA on DTLZ4. The best optimizer is MP-DEA since its median IGD values are much smaller than those of its competitors and its HV values are much larger. It is also worth noting that the performance of θ-DEA is rather robust, as it is ranked second in almost all the DTLZ4 instances.

2) Performance Comparisons on the Inverted DTLZ Test Suite: Table VI shows the median IGD and HV values on the inverted DTLZ test problems: DTLZ1^{-1}, DTLZ2^{-1}, DTLZ3^{-1}, and DTLZ4^{-1}.

For DTLZ1^{-1}, we find that MP-DEA shows better performance than the five algorithms in three- to eight-objective test instances. θ-DEA obtains the best median IGD and HV values in the ten-objective case, while VaEA has the best performance in the fifteen-objective case.

For DTLZ2^{-1}, MP-DEA is ranked first, while MOEA/D-AWA has the worst overall performance.

For DTLZ3^{-1}, MP-DEA has the best performance in five- to ten-objective problem instances in terms of IGD. MP-DEA is the best optimizer, since it achieves the best HV values in five- and eight-objective test instances. θ-DEA performs slightly worse than MP-DEA. In contrast, the performance of

TABLE V: Median obtained values of IGD and HV on the DTLZ1-4 test instances. The best and the second best results for each test instance are shown in **boldface** and underlined, respectively. The sign "+" indicates that the difference of the results is statistically significant, while the sign "-" means the opposite.

Problem	M	MP-DEA	VaEA	RVEA	MOEA/D-AWA	θ-DEA	MOEA/DD
DTLZ1	3	4.111E-2 (+ + + + +)	4.233E-2 (+ + + +)	4.116E-2 (+ + +)	5.603E-2 (+ +)	5.302E-2 (+)	**4.107E-2**
		9.87E-1 (+ + + + +)	9.73E-1 (+ + + +)	9.83E-1 (+ + +)	9.44E-1 (+ +)	9.56E-1 (+)	**9.92E-1**
	5	2.093E-1 (+ + + - +)	2.445E-1 (+ + + +)	2.332E-1 (+ + +)	3.389E-1 (+ +)	2.110E-1 (+)	**2.003E-1**
		1.00E+0 (+ + + + +)	9.89E-1 (+ + + +)	9.98E-1 (+ - +)	9.78E-1 (+ +)	9.99E-1 (+)	**1.02E+0**
	8	**1.822E-1** (+ + + + +)	2.196E-1 (+ + + +)	2.182E-1 (+ + +)	2.384E-1 (+ +)	1.830E-1 (+)	2.183E-1
		9.99E-1 (+ + + + +)	9.89E-1 (+ + + +)	9.92E-1 (+ + +)	9.84E-1 (+ +)	9.97E-1 (+)	9.94E-1
	10	**1.891E-1** (+ + - + +)	2.041E-1 (+ + + +)	1.919E-1 (+ + +)	1.893E-1 (+ +)	1.904E-1 (+)	2.866E-1
		1.11E+0 (+ + + + +)	9.95E-1 (+ + + +)	1.00E+0 (+ + +)	1.09E+0 (+ +)	1.00E+0 (+)	9.26E-1
	15	**1.754E-1** (+ + + + +)	2.186E-1 (+ + + +)	2.088E-1 (+ + +)	1.762E-1 (+ +)	2.199E-1 (+)	1.834E-1
		1.20E+0 (+ + - + +)	9.99E-1 (+ + + +)	1.00E+0 (+ + +)	1.20E+0 (+ +)	9.82E-1 (+)	1.29E-1
DTLZ2	3	**5.742E-2** (+ + + + +)	5.891E-2 (+ + + +)	5.813E-2 (+ + +)	5.933E-1 (+ +)	5.982E-2 (+)	5.764E-2
		9.42E-1 (+ + + + +)	9.23E-1 (+ + + +)	9.29E-1 (+ + +)	9.13E-1 (+ +)	9.02E-1 (+)	9.36E-1
	5	2.293E-1 (+ + + + +)	2.393E-1 (+ + + +)	2.310E-1 (+ + +)	2.301E-1 (+ +)	**2.264E-1** (+)	2.384E-1
		9.99E-1 (+ + + + +)	9.90E-1 (+ + + -)	9.91E-1 (+ + +)	9.95E-1 (+ +)	9.97E-1 (+)	9.90E-1
	8	3.628E-1 (+ + + + +)	**3.498E-1** (+ + + +)	3.512E-1 (+ + +)	4.714E-1 (+ +)	4.106E-1 (+)	3.812E-1
		9.90E-1 (+ - + + +)	**9.94E-1** (+ + + +)	9.91E-1 (+ + +)	9.77E-1 (+ +)	9.79E-1 (+)	9.88E-1
	10	4.813E-1 (+ + + + +)	**4.715E-1** (+ + + +)	5.189E-1 (+ + +)	5.709E-1 (+ +)	5.201E-1 (+)	5.111E-1
		1.00E+0 (+ + + + +)	9.99E-1 (+ + - +)	9.71E-1 (+ + +)	9.76E-1 (+ +)	9.98E-1 (+)	9.84E-1
	15	**5.810E-1** (+ + + + +)	5.993E-1 (+ + + +)	6.198E-1 (+ + +)	7.512E-1 (+ +)	6.286E-1 (+)	6.126E-1
		9.77E-1 (+ + + + +)	9.74E-1 (+ + + +)	9.55E-1 (+ + +)	9.43E-1 (+ +)	9.61E-1 (+)	9.64E-1
DTLZ3	3	**5.516E-2** (+ + + + +)	5.814E-2 (+ + + +)	5.663E-2 (+ + +)	1.297E-1 (+ +)	5.786E-2 (+)	5.536E-2
		9.48E-1 (+ + + + +)	9.38E-1 (+ + + +)	9.29E-1 (+ + +)	9.15E-1 (+ +)	9.33E-1 (+)	9.44E-1
	5	**1.718E-1** (+ + + + +)	1.987E-1 (+ + + +)	2.816E-1 (+ + +)	1.814E-1 (+ +)	2.334E-1 (+)	3.896E-1
		1.02E+0 (+ + + + +)	9.97E-1 (+ + + +)	9.76E-1 (+ + +)	9.99E-1 (+ +)	9.79E-1 (+)	9.25E-1
	8	**3.792E-1** (+ + + + +)	4.003E-1 (+ + + +)	3.819E-1 (+ + +)	3.912E-1 (+ +)	4.286E-1 (+)	5.810E-1
		9.18E-1 (+ + + + +)	9.05E-1 (+ + + +)	9.16E-1 (+ + +)	9.11E-1 (+ +)	9.03E-1 (+)	8.98E-1
	10	**4.613E-1** (+ + + + +)	4.786E-1 (+ + + +)	4.698E-1 (+ + +)	4.720E-1 (+ +)	4.791E-1 (+)	5.220E-1
		1.13E+0 (+ + + + +)	9.93E-1 (+ + + +)	1.00E+0 (+ + +)	9.96E-1 (+ +)	9.82E-1 (+)	9.72E-1
	15	6.128E-1 (+ + + + +)	6.930E-1 (+ + + +)	6.885E-1 (+ + +)	7.106E-1 (+ +)	**6.106E-1** (+)	6.230E-1
		9.92E-1 (+ + + + +)	9.73E-1 (+ + + +)	9.23E-1 (- + +)	9.23E-1 (+ +)	**9.99E-1** (+)	9.88E-1
DTLZ4	3	**5.288E-2** (+ + + + +)	1.044E-1 (+ + + +)	1.846E-1 (+ + +)	1.182E-1 (+ +)	5.340E-2 (+)	2.068E-1
		9.71E-1 (+ + + + +)	9.25E-1 (+ + + +)	9.03E-1 (+ + +)	9.13E-1 (+ +)	9.63E-1 (+)	8.98E-1
	5	**1.693E-1** (+ + + + +)	1.722E-1 (+ + - +)	1.793E-1 (+ + +)	2.382E-1 (+ +)	1.714E-1 (+)	2.528E-1
		1.15E+0 (+ + + + +)	9.92E-1 (+ + + +)	9.84E-1 (+ + +)	9.61E-1 (+ +)	1.08E+0 (+)	9.66E-1
	8	3.937E-1 (+ + + + +)	4.034E-1 (+ + + +)	3.975E-1 (+ + +)	4.962E-1 (+ +)	**3.919E-1** (+)	4.826E-1
		1.00E+0 (+ + + + +)	9.93E-1 (- + + +)	9.91E-1 (+ + +)	9.88E-1 (+ +)	9.98E-1 (+)	9.90E-1
	10	4.291E-1 (+ + + + +)	4.618E-1 (+ + + +)	**4.280E-1** (+ + +)	4.601E-1 (+ +)	4.327E-1 (+)	5.692E-1
		9.98E-1 (+ - + + +)	9.93E-1 (+ + + +)	9.97E-1 (+ + +)	9.83E-1 (+ +)	**1.00E+0** (+)	9.79E-1
	15	**4.219E-1** (+ + + + +)	4.903E-1 (+ + + +)	4.383E-1 (+ + +)	5.119E-1 (+ +)	6.214E-1 (+)	5.394E-1
		1.09E+0 (+ + + + +)	9.91E-1 (+ + + +)	1.01E+0 (+ + +)	9.76E-1 (+ +)	9.62E-1 (+)	9.73E-1

RVEA and MOEA/D-AWA is not promising.

For DTLZ4^{-1}, MP-DEA and VaEA show strong competitiveness on most of the problem instances. θ-DEA succeeds to have the best performance on the three- and five-objective cases.

3) Performance Comparisons on the WFG Test Suite: The WFG test suite is one of the most popular in the area. By testing the algorithms on the WFG test problems, we evaluate their ability in obtaining a well-converged and well-distributed set of solutions since they are characterized for presenting several complexities. Table VII presents the comparison results of MP-DEA with the other five algorithms in terms of IGD and HV values on the WFG1-9 test problems. One can notice that MP-DEA had the best performance in most cases.

The WFG1 test problem is characterized for having a mixed, biased, and scaled PF. From the empirical results presented in Table VII, it is clear that MP-DEA shows the best IGD values in the five- and fifteen-objective problem instances. VaEA obtains the best IGD value on the ten-objective instance. VaEA shows the best HV values in almost all problem instances, except for the case with five objectives. In contrast, the performance of MOEA/D-AWA is not promising.

The PF of the WFG2 test problem consists of several disconnected convex segments. MP-DEA obtains the best median IGD and HV values in the ten- and fifteen-objective WFG2 instances, while θ-DEA had the best performance on the five objective case. VaEA and MOEA/D-AWA have a similar performance in most cases.

Differently to WFG2, the PF of the WFG3 problem is

TABLE VI: Median obtained values of IGD and HV on the inverted DTLZ1-4 test instances. The best and the second best results for each test instance are shown in **boldface** and underlined, respectively. The sign "+" indicates that the difference of the results is statistically significant, while the sign "-" means the opposite.

Problem	M	MP-DEA	VaEA	RVEA	MOEA/D-AWA	θ-DEA	MOEA/DD
DTLZ1^{-1}	3	**6.368E-2** (+ + + + +)	7.352E-2 (+ + + +)	6.486E-2 (+ + +)	8.260E-2 (+ +)	8.138E-2 (+)	6.993E-2
		3.46E-1 (+ + + + +)	2.15E-1 (+ + + +)	3.22E-1 (+ + +)	1.11E-1 (+ +)	1.21E-1 (+)	2.38E-1
	5	**1.720E-2** (+ + + + +)	2.430E-1 (+ + + +)	2.186E-1 (+ - +)	1.815E-1 (+ +)	2.250E-1 (+)	3.116E-1
		3.51E-3 (+ + + + +)	9.16E-3 (+ + + +)	2.86E-3 (+ + +)	3.22E-3 (+ +)	2.12E-3 (+)	1.79E-3
	8	**2.518E-1** (+ + + + +)	2.782E-1 (+ - + +)	2.779E-1 (+ + +)	2.787E-1 (+ +)	2.613E-1 (+)	2.984E-1
		8.63E-5 (+ + + + +)	7.02E-5 (+ + + +)	6.82E-6 (+ + +)	3.86E-6 (+ +)	8.22E-5 (+)	8.12E-5
	10	2.668E-1 (+ + + + +)	3.350E-1 (+ + + +)	3.124E-1 (+ + +)	2.819E-1 (+ +)	**2.309E-1** (+)	3.981E-1
		2.89E-6 (+ + + + +)	1.98E-7 (+ + + +)	9.98E-6 (+ + +)	2.29E-6 (+ +)	**3.48E-6** (+)	2.83E-7
	15	4.633E-1 (+ + + + +)	**3.823E-1** (+ + + +)	9.901E-1 (+ + +)	5.863E-1 (+ +)	5.843E-1 (+)	9.913E-1
		1.13E-6 (+ + + + +)	**2.86E-6** (+ + + +)	6.34E-11 (+ + +)	3.67E-8 (+ +)	3.81E-7 (+)	2.66E-11
DTLZ2^{-1}	3	**7.352E-2** (+ + + + +)	7.458E-2 (+ + - +)	7.432E-2 (+ + +)	9.121E-2 (+ +)	7.460E-2 (+)	7.362E-2
		7.92E-1 (+ + + + +)	3.86E-1 (+ + + +)	4.20E-1 (+ + +)	1.28E-2 (+ +)	6.84E-1 (+)	6.91E-1
	5	**2.118E-1** (+ + + + +)	3.518E-1 (+ + + +)	3.180E-1 (+ + +)	3.236E-1 (+ +)	2.378E-1 (+)	2.980E-1
		2.46E-1 (+ + + + +)	8.23E-2 (+ + + +)	2.10E-2 (+ + +)	1.29E-1 (+ -)	1.93E-1 (+)	1.33E-1
	8	4.608E-1 (+ + + + +)	**4.218E-1** (+ + + +)	4.350E-1 (+ + +)	5.114E-1 (+ +)	5.018E-1 (+)	4.913E-1
		2.86E-3 (+ + + + -)	**3.48E-3** (+ + + +)	2.95E-3 (+ + +)	3.86E-4 (+ +)	2.23E-3 (+)	2.78E-3
	10	3.998E-1 (- + + + +)	**3.962E-1** (+ + + +)	4.337E-1 (+ + +)	4.320E-1 (+ +)	4.782E-1 (+)	4.635E-1
		1.99E-3 (+ - + + +)	**2.10E-3** (+ + + +)	1.98E-3 (+ + +)	1.83E-3 (+ +)	9.99E-4 (+)	1.61E-3
	15	**6.068E-1** (+ + + + +)	6.729E-1 (+ + + +)	6.238E-1 (+ + +)	6.523E-1 (+ +)	6.298E-1 (+)	6.114E-1
		2.95E-7 (+ + + + +)	2.14E-8 (+ + + +)	2.42E-7 (+ + +)	2.23E-8 (+ +)	1.18E-8 (+)	2.81E-7
DTLZ3^{-1}	3	6.912E-1 (+ + + + +)	7.230E-1 (+ + + +)	6.895E-1 (+ - +)	8.200E-1 (+ +)	**6.881E-1** (+)	7.196E-1
		4.36E-1 (+ + + + +)	5.27E-1 (+ + + +)	5.23E-1 (+ + +)	2.49E-2 (+ +)	**6.29E-1** (+)	6.11E-1
	5	**1.613E-1** (+ + + + +)	2.484E-1 (+ + - +)	2.627E-1 (+ + +)	2.923E-1 (+ +)	2.448E-1 (+)	2.620E-1
		3.16E-1 (+ + + + +)	1.02E-1 (+ + + +)	4.23E-2 (+ + +)	6.82E-2 (+ +)	1.13E-1 (+)	5.92E-2
	8	**3.910E-1** (+ + + + +)	6.968E-1 (- + + +)	6.978E-1 (+ + +)	4.277E-1 (+ +)	4.421E-1 (+)	4.813E-1
		4.64E-3 (+ + + + +)	1.38E-3 (+ + + +)	2.85E-3 (+ + +)	4.35E-3 (+ +)	4.23E-3 (+)	4.18E-3
	10	**4.027E-1** (+ + + + +)	4.088E-1 (+ + + +)	4.616E-1 (+ - +)	4.520E-1 (+ +)	4.619E-1 (+)	5.963E-1
		1.20E-4 (+ + + + +)	**1.23E-4** (+ + + +)	1.16E-4 (+ + +)	1.06E-4 (- +)	1.10E-4 (+)	9.96E-5
	15	5.203E-1 (+ + + + +)	5.106E-1 (+ + + +)	5.119E-1 (+ + +)	6.216E-1 (+ +)	**4.336E-1** (+)	4.838E-1
		5.63E-8 (+ + + + +)	6.38E-8 (+ + + +)	5.78E-8 (+ + +)	1.23E-8 (+ +)	**2.85E-7** (+)	1.72E-7
DTLZ4^{-1}	3	6.622E-2 (+ + + + +)	6.625E-1 (+ + + +)	7.230E-2 (+ + +)	7.282E-2 (+ +)	**6.518E-2** (+)	7.188E-2
		6.03E-1 (+ + + + +)	5.32E-1 (+ + + +)	5.13E-1 (+ + +)	4.433E-1 (+ +)	**6.32E-1**(+)	5.29E-1
	5	3.213E-1 (+ + + + +)	2.973E-1 (+ + - +)	3.998E-1 (+ + +)	3.110E-1 (+ +)	**2.971E-1** (+)	3.123E-1
		3.56E-2 (+ + + + +)	1.10E-1 (+ + + +)	4.34E-2 (+ + +)	3.84E-2 (+ +)	**1.18E-1** (+)	3.62E-2
	8	4.241E-1 (+ + + - +)	**4.223E-1** (+ + + +)	4.232E-1 (+ + +)	4.918E-1 (+ +)	4.240E-1 (+)	4.623E-1
		2.93E-3 (+ + + + +)	**3.36E-3** (+ + + +)	2.98E-3 (+ + +)	9.80E-4 (+ +)	3.13E-3 (+)	2.22E-3
	10	**1.380E-1** (+ + + + +)	1.480E-1 (+ + + +)	4.918E-1 (+ + +)	5.460E-1 (+ +)	3.328E-1 (+)	3.826E-1
		3.87E-4 (+ + + + +)	3.66E-4 (+ + - +)	2.89E-5 (+ + +)	1.23E-5 (+ +)	3.62E-4 (+)	2.49E-4
	15	**2.389E-1** (+ + + + +)	2.610E-1 (+ + + +)	6.350E-1 (+ + +)	3.274E-1 (+ +)	3.548E-1 (+)	7.278E-1
		4.13E-2 (+ + + + +)	3.79E-2 (+ + + +)	3.66E-9 (+ + +)	2.10E-2 (+ +)	1.25E-2 (+)	6.17E-10

connected. VaEA has a good overall performance on this problem, while MP-DEA succeeds to obtain the best median IGD and HV values on the ten-objective WFG3 problem instance. MOEA/D-AWA had the best median IGD and HV values on the five-objective case and the best median HV value on the fifteen-objective case.

WFG4 to WFG9 share the same PF shape in objective space, but their characteristics are different in decision space. WFG4 is known for its multi-modality, which makes an algorithm to get easily trapped in local optima. MP-DEA is ranked first since it succeeds to obtain the best overall performance in terms of HV and IGD. Both VaEA and θ-DEA have their own strong points.

For WFG5, the performance of VaEA, RVEA, MOEA/D-AWA, and MOEA/DD is worse than that of MP-DEA in the five-, ten-, and fifteen-objective cases. However, θ-DEA obtains the best median HV value on the fifteen-objective case.

The WFG6 problem is featured with a non-separable, concave, and scaled PF. MP-DEA is the best optimizer in this case. VaEA and RVEA have a similar performance on this problem. θ-DEA had the best median IGD and HV values on the five-objective case.

WFG7 is a separable and uni-modal problem. The performance of MP-DEA is significantly better than the other five algorithms. VaEA had the best performance on the ten-objective case, while MOEA/DD had the worst performance on this problem.

Similar to WFG6, WFG8 is non-separable. MP-DEA, VaEA, and θ-DEA had their own strong points on this

TABLE VII: Median obtained values of IGD and HV on the WFG1-9 test instances. The best and the second best results for each test instance are shown in **boldface** and underlined, respectively. The sign "+" indicates that the difference of the results is statistically significant, while the sign "-" means the opposite.

Problem	M	MP-DEA	VaEA	RVEA	MOEA/D-AWA	θ-DEA	MOEA/DD
WFG1	5	**1.289E-1** (+ + + + +)	2.110E+0 (+ + + +)	1.566E-1 (+ + +)	3.118E+0 (+ +)	2.631E-1 (+)	1.314E-1
		9.78E-1 (+ + + + +)	8.23E-1 (+ + + +)	9.23E-1 (+ + +)	8.00E-1 (+ +)	8.06E-1 (+)	9.67E-1
	10	1.228E-1 (- + + + +)	**1.122E-1** (+ + + +)	2.264E-1 (+ + +)	7.306E+0 (+ +)	2.141E-1 (+)	1.233E-1
		1.12E-1 (+ + + + +)	**1.17E+0** (+ + + +)	9.99E-1 (+ - +)	8.613E-1 (+ +)	9.98E-1 (+)	1.02E+0
	15	**8.293E+0** (+ + + + +)	8.230E+0 (+ + + +)	9.816E+0 (+ + +)	9.282E+0 (+ +)	1.211E+1 (+)	1.015E+1
		9.99E-1 (- + + + +)	**1.00E+0** (+ + + +)	9.96E-1 (+ + +)	9.92E-1 (+ +)	7.019E-1 (+)	7.213E-1
WFG2	5	7.409E-1 (+ + + + +)	8.112E-1 (+ + + +)	3.212E+0 (+ + +)	7.993E-1 (+ +)	**6.391E-1** (+)	8.348E-1
		9.96E-1 (+ + + + +)	9.85E-1 (+ + + -)	9.64E-1 (+ + +)	9.91E-1 (+ +)	**1.06E+0** (+)	9.81E-1
	10	**1.282E-1** (+ + + + +)	1.310E-1 (+ + + +)	1.619E+0 (+ + +)	1.349E-1(+ +)	1.296E-1 (+)	1.346E-1
		1.00E+0 (+ + + + +)	9.93E-1 (+ + + +)	7.89E-1 (+ + +)	9.78E-1 (+ +)	9.98E-1 (+)	9.82E-1
	15	**1.219E-1** (+ + + + +)	1.320E-1 (+ + + +)	1.615E-1 (+ + +)	1.642E+0 (+ +)	1.230E-1 (+)	1.648E-1
		9.87E-1 (+ + + + +)	9.75E-1 (+ + + +)	9.68E-1 (+ + +)	9.38E-1 (+ +)	9.83E-1 (+)	9.58E-1
WFG3	5	5.098E-1 (+ + + + +)	5.218E-1 (+ + + +)	5.118E-1 (+ + +)	**4.871E-1** (+ +)	7.620E-1 (+)	7.709E-1
		7.42E-1 (+ + + + +)	7.29E-1 (+ + + +)	7.33E-1 (+ + +)	**7.48E-1** (+ +)	6.82E-1 (+)	6.49E-1
	10	**1.118E-1** (+ + + + +)	1.120E-1 (+ + + +)	1.230E-1 (+ + +)	1.173E-1 (+ +)	2.386E-1 (+)	1.309E+0
		8.34E-1 (+ + + + +)	8.30E-1 (+ + + +)	8.21E-1 (+ + +)	8.24E-1 (+ +)	8.16E-1 (+)	6.82E-1
	15	**3.228E+0** (- + + + +)	3.230E+0 (+ + + +)	4.102E+0 (+ + +)	3.489E+0 (+ +)	3.560E+0 (+)	3.846E+0
		5.75E-1 (+ + + + +)	5.72E-1 (+ + + +)	5.13E-1 (+ + +)	**5.91E-1** (+ +)	5.69E-1 (+)	5.66E-1
WFG4	5	8.364E-1 (+ + + + +)	**8.320E-1** (+ + + +)	8.385E-1 (+ + +)	1.809E+0 (+ +)	8.613E-1 (+)	8.506E-1
		8.81E-1 (+ + + + +)	8.75E-1 (- + + +)	8.77E-1 (+ + +)	6.89E-1 (+ +)	8.64E-1 (-)	8.60E-1
	10	7.208E-1 (+ + + + +)	7.219E-1 (+ + + +)	8.690E-1 (+ + +)	3.862E+0 (+ +)	**6.558E-1** (+)	8.882E-1
		7.46E-1 (+ + + + +)	7.31E-1 (+ + + +)	7.24E-1 (+ + +)	6.24E-1 (+ +)	**8.03E-1** (+)	6.99E-1
	15	**6.123E-1** (+ + + + +)	6.226E-1 (+ + + +)	6.130E-1 (+ + +)	9.633E-1 (+ +)	6.320E-1 (+)	9.830E-1
		7.49E-1 (+ + + + +)	7.41E-1 (+ + + +)	7.32E-1 (+ + +)	5.42E-1 (+ +)	7.18E-1 (+)	5.27E-1
WFG5	5	**6.469E-1** (+ + + + +)	7.189E-1 (+ + + +)	9.906E-1 (+ + +)	7.227E-1 (+ -)	6.987E-1 (+)	7.230E-1
		8.53E-1 (+ + + + +)	8.26E-1 (+ + + +)	7.56E-1 (+ + +)	8.20E-1 (+ -)	8.46E-1 (+)	8.19E-1
	10	**5.928E-1** (+ + + + +)	1.613E+0 (+ + + +)	1.213E+0 (+ + +)	7.829E-1 (+ +)	5.987E-1 (+)	3.911E+0
		1.24E+0 (+ + + + +)	5.66E-1 (+ + + +)	5.23E-1 (+ + +)	1.04E+0 (+ +)	1.18E+0 (+)	4.72E-1
	15	**1.072E-1** (+ + + + +)	2.213E+0 (+ + + +)	2.110E+0 (+ + +)	4.688E+0 (+ +)	1.102E-1 (+)	1.281E+0
		5.31E-1 (+ + + + +)	4.71E-1 (+ + + +)	4.13E-1 (+ + +)	2.36E-1 (+ +)	**5.33E-1** (+)	4.56E-1
WFG6	5	7.788E-1 (+ + + + +)	9.802E-1 (+ + + +)	9.98E-1 (+ + +)	1.172E+0 (+ +)	**7.413E-1** (+)	7.641E-1
		9.73E-1 (+ + + + +)	9.26E-1 (+ + + +)	9.31E-1 (+ + +)	5.48E-1 (+ +)	**9.87E-1** (+)	9.85E-1
	10	**6.311E-1** (+ + + + +)	6.326E-1 (+ + + +)	6.403E-1 (+ + +)	6.938E-1 (+ +)	7.118E-1 (+)	7.286E-1
		8.89E-1 (+ + + + +)	8.83E-1 (+ + + +)	8.79E-1 (+ + +)	9.71E-1 (+ +)	8.56E-1 (+)	9.39E-1
	15	**8.793E+0** (+ + + + +)	8.986E+0 (+ + + +)	8.810E+0 (+ + +)	3.681E+1 (+ +)	9.386E+0 (+)	9.600E+0
		4.57E-1 (+ + + + +)	**4.63E-1** (+ + + +)	4.51E-1 (+ + +)	2.75E-1 (+ +)	3.86E-1 (+)	3.59E-1
WFG7	5	**2.260E-1** (+ + + + +)	6.829E-1 (+ + + +)	5.538E-1 (+ + +)	2.639E-1 (+ +)	2.389E-1 (+)	1.033E+0
		8.87E-1 (+ + + + +)	6.43E-1 (+ + + +)	6.64E-1 (+ + +)	8.84E-1 (+ +)	8.74E-1 (+)	2.98E-1
	10	3.512E-1 (+ + + + +)	**3.498E-1** (+ + + +)	4.118E-1 (+ + +)	6.935E-1 (+ +)	5.563E-1 (+)	2.910E+0
		9.21E-1 (- + + + +)	**9.23E-1** (+ + + +)	9.11E-1 (+ + +)	7.33E-1 (+ +)	8.86E-1 (+)	3.65E-1
	15	**8.918E+0** (- + + + +)	8.920E+0 (+ + + +)	8.936E+0 (+ + +)	9.118E+0 (+ +)	8.986E+0 (+)	1.686E+1
		3.98E-1 (- + + + +)	3.95E-1 (+ + + +)	3.81E-1 (+ + +)	3.64E-1 (+ +)	3.78E-1 (+)	2.20E-1
WFG8	5	8.890E-1 (+ + + + +)	8.970E-1 (+ + + +)	9.310E-1 (+ + +)	1.213E+0 (+ +)	**8.871E-1** (+)	9.160E-1
		7.92E-1 (+ + + - +)	7.88E-1 (+ + + +)	7.37E-1 (+ + +)	6.60E-1 (+ +)	**7.95E-1** (+)	7.42E-1
	10	7.420E-1 (+ + + + +)	**7.320E-1** (+ + + +)	7.627E-1 (+ + +)	7.784E-1 (+ +)	1.921E+0 (+)	7.864E-1
		8.41E-1 (+ + + + +)	**8.44E-1** (+ + + +)	8.38E-1 (+ + +)	8.21E-1 (+ -)	2.58E-1 (+)	8.20E-1
	15	**9.113E-1** (+ + + + +)	9.184E-1 (+ + + +)	9.326E-1 (+ + +)	5.613E+0 (+ +)	3.630E+0 (+)	6.902E-1
		9.02E-1 (+ + + + +)	8.87E-1 (+ + + +)	8.46E-1 (+ + +)	4.36E-1 (+ +)	4.62E-1 (+)	4.99E-1
WFG9	5	3.386E-1 (+ + + + +)	4.620E-1 (+ + + +)	4.133E-1 (+ + +)	9.107E-1 (+ +)	**3.337E-1** (+)	3.490E-1
		9.87E-1 (+ + + + +)	9.52E-1 (- + + +)	9.51E-1 (+ + +)	7.59E-1 (+ +)	**9.91E-1** (+)	9.79E-1
	10	**6.217E-1** (+ + + + +)	6.228E-1 (+ + + +)	6.589E-1 (+ + +)	6.920E-1 (+ +)	6.586E-1 (+)	6.789E-1
		9.27E-1 (+ + + + +)	9.14E-1 (+ + + +)	8.83E-1 (+ + +)	8.93E-1 (+ +)	8.89E-1 (+)	8.84E-1
	15	**8.123E+0** (+ + + + +)	8.389E+0 (+ + + +)	8.213E+0 (+ + +)	1.118E+1 (+ +)	3.630E+0 (+)	1.384E+1
		3.61E-1 (+ + + + +)	3.51E-1 (+ + + +)	3.58E-1 (+ + +)	2.69E-1 (+ +)	3.42E-1 (+)	2.65E-1

problem. However, MP-DEA had the best overall performance. The performance of θ-DEA was the best on the five-objective case, but it declined as the number of objectives increased.

For WFG9, MP-DEA had the best performance, while MOEA/D-AWA had the worst performance on this test problem. The empirical results on the WFG test suite show

TABLE VIII: Median obtained values of IGD and HV on MaF4-7, MaF9, and MaF12 test instances. The best and the second best results for each test instance are shown in **boldface** and underlined, respectively. The sign "+" indicates that the difference of the results is statistically significant, while the sign "-" means the opposite.

Problem	M	MP-DEA	VaEA	RVEA	MOEA/D-AWA	θ-DEA	MOEA/DD
MaF4	5	**2.588E+0** (+ + + + +)	2.749E+0 (+ + + +)	4.684E+0 (+ + +)	2.610E+0 (+ +)	3.813E+0 (+)	3.996E+0
		1.10E-1 (+ + + + +)	1.06E-1 (+ + + +)	9.96E-2 (+ + +)	1.01E-1 (+ +)	9.99E-2 (+)	9.98E-2
	10	**5.186E+1** (+ + + + +)	6.203E+1 (+ + + +)	7.473E+1 (+ + +)	7.886E+1 (+ +)	6.219E-1 (+)	2.393E+2
		2.06E-4 (+ + + + +)	1.54E-4 (+ + + +)	1.37E-6 (+ + +)	1.02E-6 (+ +)	9.67E-5 (+)	1.58E-7
	15	**2.314E+2** (+ + + + +)	4.486E+3 (+ + + +)	4.325E+3 (+ + +)	5.814E+3 (+ +)	5.361E+3 (+)	5.616E+3
		4.77E-7 (+ + + + +)	3.28E-7 (+ + + +)	3.48E-7 (+ + +)	1.29E-8 (+ +)	1.35E-8 (-)	1.35E-8
MaF5	5	2.256E+0 (+ + + + +)	2.402E+0 (+ + + +)	2.394E+0 (+ + +)	2.513E+0 (+ +)	**2.213E+0** (+)	2.483E+0
		7.75E-1 (+ + + + +)	7.64E-1 (+ + + +)	7.73E-1 (+ + +)	7.51E-1 (+ +)	**7.86E-1** (+)	7.58E-1
	10	**4.829E+1** (+ + + + +)	7.982E+1 (+ + + +)	8.586E+1 (+ + +)	8.089E+1 (+ +)	6.534E+1 (+)	1.014E+2
		9.64E-1 (+ + + + +)	9.51E-1 (+ + + +)	9.48E-1 (+ + +)	9.50E-1 (+ +)	9.53E-1 (+)	8.74E-1
	15	**1.081E+3** (+ + + + +)	3.217E+3 (+ + + +)	3.483E+3 (+ + +)	3.811E+3 (+ +)	2.533E+3 (+)	3.791E+3
		9.84E-1 (+ + + + +)	9.78E-1 (+ + + +)	9.74E-1 (+ + +)	9.56E-1 (+ +)	9.80E-1 (+)	9.68E-1
MaF6	5	**4.107E-3** (+ + + + +)	8.310E-2 (+ + + +)	9.733E-3 (+ + +)	9.314E-3 (+ +)	8.930E-2 (+)	1.964E-1
		1.28E-1 (+ + + + +)	1.24E-1 (+ + + +)	1.25E-1 (+ + +)	1.26E-1 (+ +)	1.23E-1 (-)	1.14E-1
	10	**3.183E-3** (+ + + + +)	3.213E-3 (+ + + +)	1.016E-1 (+ + +)	4.118E-3 (+ +)	5.170E-1 (+)	7.918E-1
		1.01E-1 (+ + + + +)	**1.02E-1** (+ + + +)	7.99E-2 (+ + +)	9.98E-2 (+ +)	4.32E-2 (+)	4.26E-2
	15	**9.312E-2** (+ + + + +)	9.989E-2 (+ + + +)	1.826E-1 (+ + +)	9.993E-2 (+ +)	2.063E-1 (+)	3.153E-1
		9.56E-2 (+ + + + +)	9.54E-2 (+ + + +)	8.74E-2 (+ + +)	9.36E-2 (+ +)	8.13E-2 (+)	8.54E-2
MaF7	5	3.329E-1 (+ + + + +)	4.612E-1 (+ + + +)	4.562E-1 (+ + +)	**2.934E-1** (+ +)	4.712E-1 (+)	5.320E-1
		2.52E-1 (+ + - + +)	2.50E-1 (+ + + +)	2.45E-1 (+ + +)	**2.53 E-1** (+ +)	2.37E-12 (+)	2.15E-1
	10	8.693E-1 (+ + + + +)	**8.586E-1** (+ + + +)	2.133E+0 (+ + +)	8.662E-1 (+ +)	2.818E+0 (+)	1.917E+0
		1.69E-1 (+ + + + +)	1.86E-1 (+ + + +)	1.49E-1 (+ + +)	**1.91 E-1** (+ +)	1.38E-1 (+)	1.53E-1
	15	**2.386E+0** (+ + + + +)	2.627E+0 (+ + + +)	4.031E+0 (+ + +)	6.571E+0 (+ +)	3.266E+0 (+)	2.343E+0
		1.63E-1 (+ + + + +)	1.53E-1 (+ + + -)	6.19E-2 (+ + +)	3.19E-2 (+ +)	6.14E-2 (+)	1.54E-1
MaF9	5	**1.213E-1** (+ + + + +)	1.503E-1 (+ + + +)	3.624E-1 (+ + +)	3.217E-1 (+ +)	4.010E-1 (+)	4.657E-1
		3.08E-1 (+ + + + +)	2.92E-1 (+ + + +)	1.84E-1 (+ + +)	1.90E-1 (+ +)	1.86E-1 (+)	1.81E-1
	10	1.239E-1 (+ + + + +)	**1.113E-1** (+ + + +)	1.423E-1 (+ + +)	1.214E-1 (+ +)	1.448E-1 (+)	5.936E-1
		1.67E-2 (+ + + + +)	1.65E-2 (+ + + +)	9.39E-3 (+ - +)	1.56E-2 (+ +)	9.38E-3 (+)	8.83E-3
	15	**1.276E-1** (+ + + + +)	1.477E-1 (+ + + +)	1.639E+0 (+ + +)	2.978E-1 (+ +)	1.287E+0 (+)	1.484E+0
		1.37E-3 (+ + + + +)	1.33E-3 (+ + + +)	7.34E-4 (+ + +)	1.08E-3 7 (+ +)	7.98E-4 (-)	7.98E-4
MaF12	5	1.119E+0 (+ + - + +)	1.264E+0 (+ + + +)	1.230E+0 (+ + +)	1.122E+0 (+ +)	**1.106E+0** (+)	1.284E+0
		7.33E-1 (+ + + + +)	6.92E-1 (+ + + +)	6.85E-1 (+ + +)	7.30E-1 (+ +)	**7.43E-1** (+)	6.58E-1
	10	**4.189E+0** (+ + + + +)	4.347E+0 (+ + + +)	4.574E+0 (+ + +)	4.494E+0 (+ +)	4.481E+0 (+)	4.513E+0
		8.91E-1 (+ + + + +)	8.83E-1 (+ + + +)	8.28E-1 (+ + +)	8.71E-1 (+ +)	8.72E-1 (+)	8.54E-1
	15	**6.438E+0** (+ + + + +)	6.938E+0 (+ + + +)	6.522E+0 (+ + +)	8.138E+0 (+ +)	7.013E+0 (+)	8.178E+0
		9.32E-1 (+ + + + +)	8.65E-1 (+ + + +)	9.31E-1 (+ + +)	8.51E-1 (+ +)	8.59E-1 (+)	8.52E-1

that the promising performance of MP-DEA is attributed to the MPR for balancing convergence and diversity.

4) Performance Comparisons on the MaF Test Suite: Table VIII shows the performance of the six compared algorithms in terms of median IGD and HV on the MaF4-7, MaF9, and MaF12. It can be observed that MP-DEA is ranked first among all the compared algorithms.

MaF4 is a multi-model problem with the convex PF and it is badly-scaled. It can be observed from Table VIII that MP-DEA performs best on all MaF4 test problem instances in terms of IGD and HV. VaEA and RVEA have the second best performance, while MOEA/D-AWA has the best performance in terms of IGD on the five-objective MaF4 test problem.

The Pareto-optimal set of the MaF5 test problem has a highly biased distribution, where the majority of Pareto optimal solutions are crowded in a small subregion. Besides, this test problem has a badly-scaled PF. For MaF5, one can see that MP-DEA has the best performance on the ten- and fifteen-objective MaF5 problem instances in terms of IGD and HV, while θ-DEA is ranked second.

MaF6 is designed to assess the performance of MOEAs in dealing with degenerate PFs. MP-DEA is the best optimizer, except for the ten-objective case. VaEA obtains the best median HV value in the ten-objective MaF6 instance, while MOEA/D-AWA performs better than VaEA, RVEA, θ-DEA, and MOEA/DD in the five-objective MaF6 problem instance.

MaF7 has a disconnected PF, where the number of disconnected segments is $2^M - 1$. MOEA/D-AWA shows the best IGD and HV values in the five-objective case, while MP-DEA wins in the fifteen-objective case. VaEA obtains the best IGD value in the ten-objective case.

MaF9 has a two-dimensional decision space. From the empirical results shown in Table VIII, it is clear that MP-DEA is the best optimizer where it achieves the best HV median values in all five- to fifteen-objective test instances. It also obtains the best IGD median values in the five-and fifteen-objective cases. VaEA performs slightly worse than MP-DEA.

For MaF12, its decision variables are non-separably re-

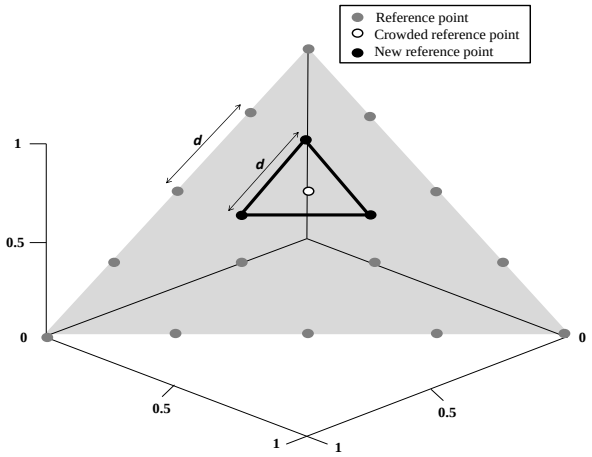

Fig. 9: The update of the set of reference points.

duced, and its fitness landscape is highly multi-modal. MP-DEA shows the best performance in MaF12, while θ-DEA outperforms in the five-objective MaF12 instance. MOEA/D-AWA and MOEA/DD show a similar performance on the MaF12 test problem.

VI. Conclusions

In this paper, we have proposed a decomposition-based algorithm for solving MaOPs with complex PFs. The environmental selection mechanism of MP-DEA is based on the MPR selection strategy. This relation employs the NBI method and the acute angle to encourage diversity, convergence, and uniformity. It also eliminates the penalty parameter θ employed in the PBI approach which varies from one problem to another [19]. The MPR is employed to compare the solutions in the same subregion. In our experimental study, we have shown that MP-DEA provides better and competitive results when compared to five recently proposed decomposition-based algorithms. In our empirical studies, we have adopted the IGD and the HV indicators to evaluate the performance of our algorithm and its counterparts on the DTLZ1-4, inverted DTLZ1-4, WFG1-9, and six MaF test problems presenting various types of difficulties involving up to fifteen objectives. The obtained results of this study indicate that our MPR is effective in solving unconstrained MaOPs with various PF shapes. However, it would be interesting to extend our proposal to solve unconstrained problems with other PF shapes [48] and constrained MaOPs by incorporating constraint-handling techniques adapted for MaOPs [29]. Moreover, applying MP-DEA to real-world problems is one of our main interests in the future [49]. In addition, it is worthwhile to investigate the performance of MP-DEA in finding only the parts of the PF that best match the DM preferences [50].

Appendix A
Update of the Reference Point Set

The description of the method that we have used to update the set of reference points is described below [29]. We first identify the crowded reference points. Then, for each one of them, we introduce a simplex of M points by setting $p = 1$. The new generated points have the same distance between two consecutive reference points on the original set of reference points. Fig. 9 illustrates an example where we have a crowded reference point in a three-objective space. In this example, three new reference points are added to the original ones. Before adding a reference point, we have to verify that it does not exist in the set of reference points and that it lies on the first quadrant.

References

[1] H. Ishibuchi, N. Tsukamoto, and Y. Nojima, "Evolutionary many-objective optimization: A short review," in *Proc. IEEE Congr. Evol. Comput. (CEC)*, Hong Kong, China, 2008, pp. 2419–2426.
[2] B. Li, J. Li, K. Tang, and X. Yao, "Many-objective evolutionary algorithms: A survey," *ACM Comput. Surveys*, vol. 48, no. 1, p. 13, Sept. 2015.
[3] S. Bechikh, M. Elarbi, and L. B. Said, "Many-objective optimization using evolutionary algorithms: A survey," in *Recent Advances in Evolutionary Multi-objective Optimization*. Springer, 2017, pp. 105–137.
[4] U. K. Wickramasinghe, R. Carrese, and X. Li, "Designing airfoils using a reference point based evolutionary many-objective particle swarm optimization algorithm," in *Proc. IEEE Congr. Evol. Comput. (CEC)*, Barcelona, Spain, 2010, pp. 1–8.
[5] G. Fu, Z. Kapelan, J. R. Kasprzyk, and P. Reed, "Optimal design of water distribution systems using many-objective visual analytics," *J. Water Resour. Plan. Manage.*, vol. 139, no. 6, pp. 624–633, Nov. 2013.
[6] P. J. Fleming, R. C. Purshouse, and R. J. Lygoe, "Many-objective optimization: An engineering design perspective," in *Proc. Int. Conf. Evol. Multi Criterion Optim. (EMO)*, Guanajuato, Mexico, 2005, pp. 14–32.
[7] K. Deb, A. Pratap, S. Agarwal, and T. Meyarivan, "A fast and elitist multiobjective genetic algorithm: NSGA-II," *IEEE Trans. Evol. Comput.*, vol. 6, no. 2, pp. 182–197, Apr. 2002.
[8] E. Zitzler, M. Laumanns, and L. Thiele, "Spea2: Improving the strength Pareto evolutionary algorithm for multiobjective optimization," in *Evolutionary Methods for Design, Optimisation and Control*, 2002, pp. 95–100.
[9] H. Ishibuchi, Y. Setoguchi, H. Masuda, and Y. Nojima, "Performance of decomposition-based many-objective algorithms strongly depends on Pareto front shapes," *IEEE Trans. Evol. Comput.*, vol. 21, no. 2, pp. 169–190, Apr. 2017.
[10] A. López Jaimes and C. A. C. Coello, "Some techniques to deal with many-objective problems," in *Proc. 11th Annu. Conf. Genet. Evol. Comput. (GECCO)*, Montreal, Québec, Canada, 2009, pp. 2693–2696.
[11] K. Deb and H. Jain, "An evolutionary many-objective optimization algorithm using reference-point-based nondominated sorting approach, part I: Solving problems with box constraints," *IEEE Trans. Evol. Comput.*, vol. 18, no. 4, pp. 577–601, Aug. 2014.
[12] Q. Zhang and H. Li, "MOEA/D: A multiobjective evolutionary algorithm based on decomposition," *IEEE Trans. Evol. Comput.*, vol. 11, no. 6, pp. 712–731, Dec. 2007.
[13] K. Li, K. Deb, Q. Zhang, and S. Kwong, "An evolutionary many-objective optimization algorithm based on dominance and decomposition," *IEEE Trans. Evol. Comput.*, vol. 19, no. 5, pp. 694–716, Oct. 2015.
[14] M. Elarbi, S. Bechikh, A. Gupta, L. B. Said, and Y.-S. Ong, "A new decomposition-based NSGA-II for many-objective optimization," *IEEE Trans. Syst., Man, Cybern., Syst.*, vol. 48, no. 7, pp. 1191–1210, Jul. 2018.
[15] M. Garza-Fabre, G. Toscano-Pulido, C. A. C. Coello, and E. Rodriguez-Tello, "Effective ranking+ speciation= Many-objective optimization," in *Proc. IEEE Congr. Evol. Comput. (CEC)*, New Orleans, LA, USA, 2011, pp. 2115–2122.
[16] V. Khare, X. Yao, and K. Deb, "Performance scaling of multi-objective evolutionary algorithms," in *Proc. Int. Conf. Evol. Multi Criterion Optim. (EMO)*, Faro, Portugal, 2003, pp. 376–390.
[17] R. C. Purshouse and P. J. Fleming, "Evolutionary many-objective optimisation: An exploratory analysis," in *Proc. IEEE Congr. Evol. Comput. (CEC)*, vol. 3, Canberra, ACT, Australia, 2003, pp. 2066–2073.
[18] Y. Xiang, Y. Zhou, M. Li, and Z. Chen, "A vector angle-based evolutionary algorithm for unconstrained many-objective optimization," *IEEE Trans. Evol. Comput.*, vol. 21, no. 1, pp. 131–152, Feb. 2017.

[19] H. Ishibuchi, N. Akedo, and Y. Nojima, "Behavior of multiobjective evolutionary algorithms on many-objective knapsack problems," *IEEE Trans. Evol. Comput.*, vol. 19, no. 2, pp. 264–283, Apr. 2015.

[20] A. Mohammadi, M. N. Omidvar, X. Li, and K. Deb, "Sensitivity analysis of penalty-based boundary intersection on aggregation-based EMO algorithms," in *Proc. IEEE Congr. Evol. Comput. (CEC)*, Sendai, Japan, 2015, pp. 2891–2898.

[21] J. Guo, S. Yang, and S. Jiang, "An adaptive penalty-based boundary intersection approach for multiobjective evolutionary algorithm based on decomposition," in *Proc. IEEE Congr. Evol. Comput. (CEC)*, Vancouver, BC, Canada, 2016, pp. 2145–2152.

[22] J. Zou, L. Fu, J. Zheng, S. Yang, G. Yu, and Y. Hu, "A many-objective evolutionary algorithm based on rotated grid," *Applied Soft Computing*, vol. 67, pp. 596–609, Jun. 2018.

[23] K. Deb, L. Thiele, M. Laumanns, and E. Zitzler, "Scalable multi-objective optimization test problems," in *Proc. IEEE Congr. Evol. Comput. (CEC)*, vol. 1, Honolulu, HI, USA, 2002, pp. 825–830.

[24] S. Huband, P. Hingston, L. Barone, and L. While, "A review of multiobjective test problems and a scalable test problem toolkit," *IEEE Trans. Evol. Comput.*, vol. 10, no. 5, pp. 477–506, Oct. 2006.

[25] R. Cheng, M. Li, Y. Tian, X. Zhang, S. Yang, Y. Jin, and X. Yao, "A benchmark test suite for evolutionary many-objective optimization," *Complex & Intelligent Systems*, vol. 3, no. 1, pp. 67–81, 2017.

[26] K. Miettinen, *Nonlinear multiobjective optimization*. Springer Science & Business Media, 2012, vol. 12.

[27] M. Asafuddoula, H. K. Singh, and T. Ray, "An enhanced decomposition-based evolutionary algorithm with adaptive reference vectors," *IEEE Trans. Cybern.*, vol. 48, no. 8, pp. 2321–2334, Aug. 2018.

[28] Y. Qi, X. Ma, F. Liu, L. Jiao, J. Sun, and J. Wu, "MOEA/D with adaptive weight adjustment," *Evol. Comput.*, vol. 22, no. 2, pp. 231–264, 2014.

[29] H. Jain and K. Deb, "An evolutionary many-objective optimization algorithm using reference-point based non-dominated sorting approach, part II: Handling constraints and extending to an adaptive approach," *IEEE Trans. Evol. Comput.*, vol. 18, no. 4, pp. 602–622, Aug. 2014.

[30] H.-L. Liu, L. Chen, Q. Zhang, and K. Deb, "An evolutionary many-objective optimisation algorithm with adaptive region decomposition," in *Proc. IEEE Congr. Evol. Comput. (CEC)*, Vancouver, BC, Canada, 2016, pp. 4763–4769.

[31] R. Wang, R. C. Purshouse, and P. J. Fleming, "Preference-inspired co-evolutionary algorithms using weight vectors," *Eur. J. Oper. Res.*, vol. 243, no. 2, pp. 423–441, 2015.

[32] Hua, Yicun and Jin, Yaochu and Hao, Kuangrong, "a clustering-based adaptive evolutionary algorithm for multiobjective optimization with irregular Pareto fronts," *IEEE Trans. Cybern.*, no. 99, pp. 1–13, Jun. 2018.

[33] Ge, Hongwei and Zhao, Mingde and Sun, Liang and Wang, Zhen and Tan, Guozhen and Zhang, Qiang and Chen, CL Philip, "a many-objective evolutionary algorithm with two interacting processes: Cascade clustering and reference point incremental learning," *IEEE Trans. Evol. Comput.*, pp. 1–1, Oct. 2018.

[34] Jiang, Shouyong and Yang, Shengxiang, "an improved multiobjective optimization evolutionary algorithm based on decomposition for complex Pareto fronts," *IEEE Trans. Cybern.*, vol. 46, no. 2, pp. 421–437, Mar. 2016.

[35] Wu, Mengyuan and Li, Ke and Kwong, Sam and Zhang, Qingfu and Zhang, Jun, "learning to decompose: a paradigm for decomposition-based multiobjective optimization," *IEEE Trans. Evol. Comput.*, pp. 1–1, Aug. 2018.

[36] I. Giagkiozis, R. C. Purshouse, and P. J. Fleming, "Towards understanding the cost of adaptation in decomposition-based optimization algorithms," in *IEEE International Conference on Systems, Man and Cybernetics (SMC)*. IEEE, 2013, pp. 615–620.

[37] I. Das and J. E. Dennis, "Normal-boundary intersection: A new method for generating the Pareto surface in nonlinear multicriteria optimization problems," *SIAM J. Optim.*, vol. 8, no. 3, pp. 631–657, 1998.

[38] Y. Yuan, H. Xu, B. Wang, and X. Yao, "A new dominance relation-based evolutionary algorithm for many-objective optimization," *IEEE Trans. Evol. Comput.*, vol. 20, no. 1, pp. 16–37, Feb. 2016.

[39] K. Deb and R. B. Agrawal, "Simulated binary crossover for continuous search space," *Complex Syst.*, vol. 9, no. 3, pp. 1–15, 1995.

[40] K. Deb and M. Goyal, "A combined genetic adaptive search (geneas) for engineering design," *Comput. Sci. Informat.*, vol. 26, no. 4, pp. 30–45, 1996.

[41] C. A. C. Coello, G. B. Lamont, D. A. Van Veldhuizen *et al.*, *Evolutionary algorithms for solving multi-objective problems*. Springer, 2007, vol. 5.

[42] E. Zitzler and L. Thiele, "Multiobjective evolutionary algorithms: A comparative case study and the strength Pareto approach," *IEEE Trans. Evol. Comput.*, vol. 3, no. 4, pp. 257–271, Nov. 1999.

[43] J. Bader and E. Zitzler, "Hype: An algorithm for fast hypervolume-based many-objective optimization," *Evol. Comput.*, vol. 19, no. 1, pp. 45–76, Mar. 2011.

[44] L. While, L. Bradstreet, and L. Barone, "A fast way of calculating exact hypervolumes," *IEEE Trans. Evol. Comput.*, vol. 16, no. 1, pp. 86–95, Feb. 2012.

[45] J. J. Durillo and A. J. Nebro, "jmetal: A java framework for multi-objective optimization," *Advances in Engineering Software*, vol. 42, no. 10, pp. 760–771, 2011.

[46] F. Wilcoxon, "Individual comparisons by ranking methods," *Biometrics Bulletin*, vol. 1, no. 6, pp. 80–83, Dec. 1945.

[47] R. Cheng, Y. Jin, M. Olhofer, and B. Sendhoff, "A reference vector guided evolutionary algorithm for many-objective optimization," *IEEE Trans. Evol. Comput.*, vol. 20, no. 5, pp. 773–791, Oct. 2016.

[48] Q. Zhang, A. Zhou, S. Zhao, P. N. Suganthan, W. Liu, and S. Tiwari, "Multiobjective optimization test instances for the CEC 2009 special session and competition," *University of Essex and Nanyang Technological University, Technical Report. CES-487*, vol. 264, 2008.

[49] T. W. Simpson, W. Chen, J. K. Allen, and F. Mistree, "Conceptual design of a family of products through the use of the robust concept exploration method," in *AIAA/USAF/NASA/ISSMO Symposium on Multidisciplinary Analysis and Optimization*, vol. 2, 1996, pp. 1535–1545.

[50] K. Deb and A. Kumar, "Light beam search based multi-objective optimization using evolutionary algorithms," in *Proc. IEEE Congr. Evol. Comput. (CEC)*, Singapore, Singapore, 2007, pp. 2125–2132.